

We are grateful to the editor and reviewers for their time and constructive comments to improve this manuscript. Here we address our reply point by point, in bold font. Both editor's and reviewer's comments are in regular font. All changes are marked with red or green in the revised manuscript.

Editor Decision: Publish subject to minor revisions (Editor review) (18 May 2016) by Andreas Vieli

Comments to the Author:

Editor decision after reviews of revised revision.

Dear X. Wang et al,

The revised version of the manuscript was sent to 2 reviewers again (comments further below), and although they both indicated that the revised version has improved to some degree (compared to the original submission) they both stated that the general writing and English language clearly need further improvement, a point that I also made to you after the first revised version of the manuscript. I then already asked you to carefully edit and correct the whole document again, and not just the few points that I spotted. It is really not the job of the reviewers to correct the manuscript for English language grammatical errors, irregular punctuation, and awkward phrasing, but the author's. Both reviewers seemed rather disappointed regarding this aspect of the revised version.

Reviewer 2 had beside the English languages issues some rather minor further points to address (see list of reviewer 2), of which some concern the definitions/explanation (e.g. sea floor elevation, E_sf) in the methods.

Reviewer 1 was less positive and had besides the major language issues some rather substantial remaining issues concerning the methods and presentation (see major comments by reviewer 1) and on this basis recommended to reject this paper. As an editor I agree in principle with some of the more substantial points made by reviewer 1 but I think they are relatively easy to be addressed by the authors and do not fully justify a rejection.

So, I suggest to the authors to very carefully address the

(i) To very carefully address ALL the minor comments and points listed by the reviewers 1 and 2

Reply: We have revised the manuscript thoroughly according to comments from both reviewers. All changes are marked with red or green in the revised manuscript.

(ii) Re-check and correct the ENTIRE publication again VERY CAREFULLY for English language, grammatical errors, awkward phrasing and small editing issues. I advise you to get the whole document checked again at the end by a native English speaker.

Reply: We read and check the manuscript thoroughly again and the changes are marked with red or green in this revision.

(ii) To address the following more substantial points (a-d) by reviewer 1:

(a) Reviewer 1 is concerned about the calculation of E_{dif} below the substantive areas of MIT where no bathymetric data are available (only extra/interpolated). While such an E_{dif} can (theoretically) be calculated using the interpolated bathymetric data, I agree with the reviewer that it has not that much meaning other than based on the interpolated data (and other indicators) it is likely that MIT is floating there. There is a supplementary figure now showing where there is actually bathymetric data which helps regarding this aspect, but I would try to make this point a bit clearer in the main paper. There are a variety of ways to do this, here some suggestions:

-Provide the justification and all the available evidence for believing 'that the tongue is floating' rather than to carry out and show the entire calculation for E_{dif} based on extrapolated sea-floor heights.

-or clearly mark in fig 3 and in fig 6 (maybe with black hatching or similar) the areas where there is no bathymetric data available (or is just extrapolated).

-or show supplementary figure 1a) as Figure 3b).

Whatever option is taken, in the text it should be made clearer that the E_{dif}

Reply: We agree with you on this point. We take up your third suggestion and the S-Fig 1a and S-Fig 1b from last revision is moved to the text as Fig 3b and Fig 3c. In this way, the spatial distribution of bathymetry is clearer.

(b) regarding the detection of grounding from E_{dif} : I agree with reviewer 2 that the statement on line 340/341 of '... E_{dif} less than 23 m corresponds to a very robust grounding event...' seems not quite right and also not consistent with the figures and interpretation in section 5 (line 353: E_{dif} less than 23m interpreted as 'almost grounded'). Maybe there is just a minus sign missing in front of 23m on line 340, I think it should say: below -23m it seems very strongly grounded, between -23m and 23m slightly grounded and above 23m unlikely to be grounded. Please check this carefully and adjust accordingly in whole document.

Reply: We agree with you on this point. E_{dif} below -23 m should be strongly grounded. We have revised the manuscript thoroughly according to this comment.

(c) Address the more structural issues (methodological explanations to the methods, discussion points to discussion (see detailed comments by reviewer 2).

Reply: We have revised the manuscript thoroughly according to comments from both reviewers.

(d) Clarify the point on applying the firn-air content calculation on heavily grounded ice bergs. I assume although you use 'heavily' grounded they are still very close to floatation but hardly move and hence floatation still is applicable.

Reply: We didn't use "heavily grounded" icebergs for FAC calculation. Because the icebergs we chose could still move slowly, as can be seen from S-Fig. 1. We consider they are still close to floatation. The hydrostatic equilibrium still applies for these icebergs. "Heavily" was only

used to describe the B-9B iceberg which stayed in a point for several years. We have checked the manuscript thoroughly to make sure proper description on these icebergs.

Thank you and best regards

Andreas Vieli

The editor

18 May 2016

Comments Reviewer 1:

This is my second review of this paper. I am somewhat disappointed with the revisions, in that one of the key points in my, and the other reviewer's, review was that the paper needed careful editing by the authors before it would be publishable. It appears that some of the edits suggested by the reviewers and the editor are included in this version, but that the authors have not found the grammatical errors, irregular punctuation, and awkward phrasing that were not specifically identified during the first review process. These remain in the present manuscript and it is the authors' responsibility to correct them.

Reply: We have revised the manuscript thoroughly according to your comments. All changes are marked with red or green in the revised manuscript.

The paper also remains somewhat disorganized. The discussion section contains material that belongs in the methods section, and the results section contains material that belongs in the discussion section. I have made some notes to this effect, but the authors should revise the paper carefully to make sure that each section contains only the appropriate material.

Reply: We have made proper changes on structure and revised the manuscript thoroughly according to your comments.

For the scientific content of the paper, I am concerned to see that the authors are still presenting their calculation of E_{dif} under the MIT in areas where there are no measurements of bathymetry. There is a small area near the northwest edge of the tongue where the MIT has overrun some measured bathymetry, and in these areas it is appropriate to calculate E_{dif} , but for the rest of the tongue, it seems cleaner to provide a justification for believing that the tongue is floating than to carry out the calculation based on extrapolated sea-floor heights.

Reply: In the last revision, we used the ice tongue boundary from 2000 to identify the data gaps. One can easily identify the data gaps using this boundary. To better illuminate the spatial distribution of bathymetry, we have moved the S-Fig. 1 in the last revision to text as Fig. 3b and Fig. 3c by taking up Editor's suggestion.

The firn-air content calculation does not seem very useful. To calculate the firn air, the authors must use a point where the bathymetry is known, so that the ice bergs are grounding. But if the bergs are grounded, the hydrostatic approximation does not apply.

Reply: The FAC calculation is useful to invert the ice draft and ice bottom elevation. We did select the icebergs located in region with bathymetry known, as can be seen from Fig. 3b. Although some icebergs were chosen as slightly grounding, they still moved slowly. From this point of view, hydrostatic approximation still applies.

Last, the authors seem to have the detection limits for their grounding detection wrong. E_{dif} is equal to the inferred elevation of the ice bottom minus the sea floor. Suppose sea floor is known to be at -500 m, and the bottom of the ice berg is inferred to be at -524 m, give or take 23 m. Then $E_{diff} = -24$, with a one-sigma range between -47 and -1 meters. Likewise, if the bottom of the ice

berg is inferred to be at -478 m, give or take 23 m, then $E_{diff} = +22$, with a 1-sigma range between -1 and 45 meters. The first case represents robust grounding, the second case In section 6, the authors say :

“ E_{diff} less than 23 m corresponds to a very robust grounding event”.

A robust grounding event should be one where the one-sigma range is entirely below zero (my first case) while a plausible, but not robust, grounding even is one where the one-sigma range includes zero, but also includes positive values (my second case). If E_{diff} is greater than 23 m, then at one sigma you can be confident that there is no grounding.

Reply: We agree with you on this point. To make it further clearer, we add some sentences in the text. We take up Editor’s suggestion and the standard to tell grounding or floating of an iceberg using E_{diff} is: below -23m very strongly grounded, between -23m and 23m slightly grounded and above 23m unlikely to be grounded. We have revised the manuscript thoroughly according to this comment.

87, Delete sentence beginning “With billions...” The other data types are not relevant here.

Reply: We think that it is proper to keep it so readers can know there are different products from ICESat/GLAS and what data we are using for this study.

132- This seems wrong. Clouds cannot cause ICESAT saturation.

Reply: We change “the occurrence of clouds” to “high reflected natural surface”.

136: You subtract off TPX07.1, but do you reapply it in the freeboard calculation? The freeboard is the ice surface height minus the sea-surface height, and if you don’t use a tide model, the tidal elevation causes an error.

Reply: We had made it very clear in the last revision that we use instantaneous sea surface height to extract the freeboard. This is correct because freeboard is distance from ice top to sea surface, not sea level. The instantaneous sea surface height varies with tide, thus no need to consider the tide height.

138-139: Not sure what this means. Please explain or delete.

Reply: Elevation we used is usually referred to a geoid or ellipsoid. This sentence is to introduce the elevation we used in this study. The full name of WGS-84 and EGM08 can be found from line 105 to line 106. In this revision, we keep it unchanged in this revision and one reference is added on EGM08 in line 117.

158-166: How are height gradients taken into account in this calculation? For a sloping surface, relocating the footprints by the ice velocity will introduce a spurious elevation change signal.

Reply: Because of sloping surface of the MIT, sloping error caused by footprint relocation must be considered and put into the final error sources. In this study, the contribution of

footprint relocation to freeboard uncertainty is calculated as “ Δd ” multiplying “ Δs ”, where “ Δd ” is the relocation error caused by the uncertainty of ice flow, “ Δs ” the average surface slope of the MIT.

170: These equations need to be placed immediately after their introductory sentence. I suggest deleting the reference at 165 to these equations and adding one sentence such as “The corrected positions of the footprints are:” at 170.

Reply: We take up your suggestion and move the equations 2 and 3 ahead so they connect to line 165 directly. We keep other description unchanged.

179: don't need to discuss interpolation techniques not used here.

Reply: We delete the sentence in this revision.

186: Put equation 4 here, not eight lines below.

Reply: We move equation 4 just after this sentence.

253-56: How are the PIG icebergs relevant here? I suggest deleting the reference.

Reply: We take up your suggestion and delete it in this revision.

266-68: If the iceberg is grounded, then the bed is supporting some part of its weight. This means that it is not in hydrostatic equilibrium: $\rho_w D < \rho_i (H_f + D - FAC)$. This seems to introduce a potentially large error into your calculation of FAC.

Reply: We use “grounded” to describe the iceberg used for FAC calculation in the last revision because they moved slowly compared free drifting icebergs. However those icebergs could move as can be seen from S-Fig 1 which indicates that they are still very close to floatation and flotation still is applicable. We change “grounded” to “slightly grounded” in this revision when describing these icebergs used for FAC calculation.

265-270: Are you using all the ice bergs, or only the 2006 measurements? If the latter, is this a least-squares calculation, or just a simple solution?

Reply: We use the 2006 measurements to invers the FAC which was clearly addressed in line 263-266: “In this study, only the top two largest freeboard measurements of icebergs ‘A’ and ‘C’ from T1289 in 2006 are employed to calculate the FAC with Eq. (7) with a least-squares method under hydrostatic equilibrium”. Because four equations were created, FAC is a least-squares solution.

331: 50 times 0.00024 is 0.012. This is not a realistic estimate of the surface slope due to rugged, crevassed ice-tongue surfaces.

Reply: The average slope of MIT was calculated as 0.00024 (Wang et al. 2014). In this study, we have already magnified it by 50 times. Because we want to explore the average contribution to grounding detection from footprint relocation by considering ice velocity

uncertainty and average surface slope, not under an extreme situation, we feel this is a reasonable approach for the ice front treatment. The freeboard error caused by our approach is reasonable and we kept our original approach in the revised manuscript.

384-395: this material belongs in the 'Discussion' section.

Reply: Done.

Section 6.1:

Why does it make sense to talk about the area rate rather than the longitudinal flow rate? The mechanism proposed for interaction between MIT and the Mertz bank is that the MIS should break after it hits the bank. The time for the MIT to reach the bank after it calves is then distance between the end of the MIT and the bank divided by the speed of the end of the tongue. Casting this in terms of area seems to make the calculation more confusing, and is not clearly more accurate.

Reply: We did not mean that MIT should break once it hits the Mertz Bank. Instead this is a slow progress, that's why we use the maximum ice tongue area and area rate to calculate the calving cycle. As can be seen from Massom et al. (2015), large rift could occur because of this hit and only the large rift propagates to the other flank can the ice tongue break off.

Section 6.2: Most of this material belongs in the 'methods' section, where you should explain the limitations of, and the rationale for, your methods. It also sounds here like you are solving for the FAC using only the 2006 ice-berg heights, while before it sounded like you were including all the data in a least-squares calculation.

Reply: Section 6.2.1 about the lowest sea surface height extraction is moved to method. Section 6.2.2 about FAC extraction is moved to section 3.2. For FAC calculation, we have made it very clear in line 263-266 in the last revision: "In this study, only the top two largest freeboard measurements of icebergs 'A' and 'C' from T1289 in 2006 are employed to calculate the FAC with Eq. (7) with a least-squares method under hydrostatic equilibrium". We keep this consistent throughout the manuscript.

484: The discussion of the accuracy of the bathymetry belongs in the data section.

Reply: The first paragraph about the accuracy of bathymetry is moved to the data section. However the other paragraphs about interpolation error are not proper to be moved to the data section, which are still kept in the discussion.

497: Talking about the accuracy of the seafloor DEM under MIT makes little sense, because there are no measurements there, and the values provided are extrapolated/interpolated from measurement locations that are often far away. The arguments (503 - 517) that the bulk of MIS is floating are a better approach than making unfounded assumptions about the height of the bed where no data are available.

Reply: This paragraph started from line 497 is removed in this revision.

Figure 3: There are too many colors here. The bathymetry needs to be in a color scale that does not overlap the colors chosen for the outlines. Consider grayscale.

Reply: Figure 3 is redrawn and grayscale is used for seafloor topography.

Figure 6: Indicate clearly the areas in which the seafloor elevations are constrained by data. Do not show E_{diff} where they are not.

Reply: We move S-Figure 1 to the text as Fig. 3b and Fig. 3c so that the spatial distribution of bathymetric measurements is clear.

Figure 9: this figure is out of order, and is probably unnecessary.

Reply: We want to use this figure to show freeboard of the icebergs and we added this figure in the last revision because reviewer 2 wanted us to show more about the iceberg freeboard. In this revision, we move this figure to supplementary.

Comments Reviewer 2:

The incorporated revisions have considerably improved the manuscript. A few minor revisions are listed below.

line 29: Replace “The calving of MIT can be cyclical because...” with “In the calving induced by iceberg collisions, our observations suggest that calving of the MIT is a cyclical process controlled by the presence...”

Reply: Done.

line 40: Change “... Mertz polynya, and sea-ice production and dense, shelf-water formation” to “...Mertz polynya, sea ice production, and dense shelf water formation...”

Reply: Done.

line 47: Change “how severe the grounding was” to something like “the extent of grounding” or possibly even “the severity of grounding”

Reply: Done.

line 60-61: This is a somewhat odd sentence “Grounding as a potential factor can affect the stability of an ice tongue...”. I would suggest that you revise and rephrase to indicate how grounding can affect ice tongue stability, not just state that it can influence stability.

Reply: we change it to “Grounding as a potential factor can affect the stability of an ice tongue by possibly holding the tongue to delay calving (Massom et al. 2015)” in this revision.

line 77: “launched” not “lunched”

Reply: Done.

line 130: Change to “The first step involves data processing...”

Reply: Done.

lines 134-135: “... are corrected following the procedures in Wang et al. (2012, 2013).”

Reply: Done.

line 137: If I’m interpreting this correctly, change to “... to obtain estimates of the instantaneous sea surface height.” You talk about extracting sea surface elevations in the next paragraph, however, so I’m not sure that’s what you mean here.

Reply: we change it to “Furthermore, tidal correction from the TPX07.1 tide model in GLA12 data record is removed to obtain estimates of the instantaneous sea surface height”. Also we change “sea level” to “sea surface height” thoroughly in this revision because we use the instantaneous measurements of sea surface height which is not “sea level”.

line 139: How are the data prepared for use?

Reply: we change it to “Finally, elevation data related to the WGS-84 ellipsoid and EGM 08 geoid for ICESat/GLAS from 2003 to 2009 is ready for subsequent use.”

line 150: What do you mean by “almost repeatedly”?

Reply: ICESat/GLAS did not have an exactly repeated ground track. For the same track, ground measurements can bias by several tens to several hundred meters in cross-track direction. That is why we use “almost repeatedly”.

line 156: “For example, consider ICESat data from...”

Reply: Done.

line 158: “... distance between track T165 and T31 is ~7.5 km without accounting for ice advection between observation dates.”

Reply: Done.

line 170: Remove “a little”

Reply: Done.

line 184: Replace “because of known ice tongue outlines from Landsat images” to “when the ice tongue outline can be delineated from Landsat images”

Reply: Done.

line 186: “... assuming hydrostatic equilibrium and using the lowest sea-surface height (further discussed in section 6.2.2), which is extracted from ICESat/GLAS data...”

Reply: Done.

line 201: Remove “at”

Reply: Done.

line 209: You don’t need to define Edif here since you just defined it before the equation but you need to define Esf (which I assume is the sea floor elevation).

Reply: Done.

line 213-214: The author’s name is “van den Broeke”

Reply: Done.

line 228: “that will influence the density of the ice tongue” rather than “that makes ice mass calculation complicated”

Reply: Done.

line 311: “compared with interpolated freeboard estimates”

Reply: Done.

line 325: Add a reference for the inter-campaign uncertainty in ICESat data

Reply: We change it to “we use ± 0.15 m (Zwally et al. 2002) as the uncertainty of elevation data (ϵE_s)” in this revision.

line 372: I recommend changing “was grounded more significantly” to “became more firmly grounded” because you aren’t performing any statistical tests.

Reply: Done.

lines 399-400: Remove one of the “over this period”

Reply: Done.

line 411: End line 410 with a period after the reference then start a new sentence explaining that, based on your observations, you think only one large calving event occurred. (“Based on the interactions between the Mertz ice tongue and Mertz Bank suggested by our observations and described below, it is likely that only one large calving event occurred between 1912-29156.”)

Reply: Done.

line 425: “Because of the continuous advection of ice from upstream and the fixed location of the shallow Mertz Bank, the calving is...”

Reply: Done.

line 434: Of “the” Mertz polynya.

Reply: Done.

line 439-441: Why would a shorter ice tongue lead to a reduction in katabatic winds (which are driven by air temperature and pressure gradients over steep grounded ice) and polynya size? Elaborate.

Reply: We did not mean that a shorter ice tongue leads to a reduction of katabatic winds. However we mean that a shorter ice tongue leads to a small polynya size formed by katabatic wind. Different length of an ice tongue can block sea ice drifting from one side differently. A long MIT help to maintain a large polynya because more sea ice formed on the east side could not drift to the west side. With the effect of katabatic wind, sea ice produced from the west side is blown seaward. In this revision, we make this point much clear by explaining more.

line 443: “Mertz wellwhich”?

Reply: There should be a space between “well” and “which”. We change it to “...Mertz well which...” in this revision.

lines 512-514: I’m not sure I follow this. Why does the absence of shadowing (of ice, the ocean, ???) indicate flotation?

Reply: To avoid confusion, we delete these sentences.

Figure 3: Change the color and/or relative position of the dashed-dotted line so that it is easier to discern.

Reply: Figure 3 is redrawn and grayscale is used for seafloor topography.

1 **Grounding and Calving Cycle of Mertz Ice Tongue**

2 **Revealed by Shallow Mertz Bank**

3 Xianwei Wang^{1,2}, David M. Holland^{2,3}, Xiao Cheng^{1,5} and Peng Gong^{4,5}

4 1. State Key Laboratory of Remote Sensing Science, and College of Global Change and Earth System Science,

5 Beijing Normal University, Beijing 100875, China.

6 2. Center for Global Sea Level Change, New York University Abu Dhabi, Abu Dhabi, United Arab Emirates.

7 3. Courant Institute of Mathematical Sciences, New York University, New York 10012, United States of America.

8 4. Ministry of Education Key Laboratory for Earth System Modeling, and Center for Earth System Science,

9 Tsinghua University, Beijing, China 100084.

10 5. Joint Centre for Global Change Studies, Beijing, China.

11
12 *Correspondence to: wangxianwei0304@163.com*

13 **Abstract**

14 A recent study, using remote sensing, provided some evidence that a seafloor shoal
15 influenced the 2010 calving event of the Mertz Ice Tongue (MIT), by partially grounding the
16 MIT several years earlier. In this paper, we start by proposing a method to calculate Firn Air
17 Content (FAC) around Mertz from seafloor-touching icebergs. Our calculations indicate the FAC
18 around Mertz region as 4.87 ± 1.31 m. We then design an indirect method of using freeboard and
19 ~~sea level~~sea surface height data extracted from ICESat/GLAS, FAC, and relatively accurate
20 seafloor topography to detect grounding sections of the MIT between 2002 and 2008 and analyze
21 the process of grounding prior to the calving event. By synthesizing remote sensing data, we
22 point out that the grounding position was localized northeast of the Mertz ice front close to the
23 Mertz Bank. The grounding outlines of the tongue caused by the Mertz Bank are extracted as
24 well. From 2002 to 2008, the grounding area increased and the grounding became more
25 pronounced. Additionally, the ice tongue could not effectively climb over the Mertz Bank in
26 following the upstream ice flow direction and that is why MIT rotated clockwise after late 2002.
27 Furthermore, we demonstrate that the area-increasing trend of the MIT changed little after
28 calving ($\sim 36 \text{ km}^2/\text{a}$), thus allowing us to use remote sensing to estimate the elapsed time until the
29 MIT can reground on and be bent by the shoal. This period is approximately 70 years. ~~The~~
30 ~~calving of MIT can be cyclical because~~ In the calving induced by iceberg collisions, our
31 observations suggest that calving of the MIT is a cyclical process controlled by the presence of
32 the shallow Mertz Bank location and the flow rate of the tongue. The calving cycle of the MIT
33 explains the cycle of sea-surface condition change around the Mertz.

34 **Keywords:** Mertz Ice Tongue, firn air content, ~~iceberg~~ grounding, Mertz Bank, calving cycle.

35 **1. Introduction**

36 Surface-warming induced calving or disintegration of floating ice has occurred in
37 Antarctica, such as the Larsen B ice shelf (Scambos et al., 2000, 2003; Domack et al., 2005;
38 Shepherd et al., 2003). While surface or sub-surface melting has largely been recognized to
39 contribute to floating ice loss in Antarctica (Depoorter et al., 2013), calving caused by interaction
40 with the seafloor has not been widely considered. The Mertz Ice Tongue (MIT) was reported to
41 have calved in 2010, subsequent to being rammed by a large iceberg, B-9B (Legresy et al. 2010).
42 After the calving, the areal coverage of the Mertz polynya, ~~and~~ sea-ice production and dense,
43 shelf-water formation in the region changed (Kusahara et al. 2011; Tamura et al. 2012).
44 However, the iceberg collision may have only been an apparent cause of the calving as other
45 factors had not been fully considered such as seafloor interactions (Massom et al., 2015; Wang.
46 2014). By comparing inverted ice thickness to surrounding bathymetry, and combining remote
47 sensing, Massom et al., (2015) considered that the seabed contact may have held the glacier
48 tongue in place to delay calving by ~8 years. The interaction of the MIT with the seafloor, the
49 exact grounding location of the MIT before calving and ~~how severe~~ the extent of grounding ~~was~~
50 are still not well-known.

51 The MIT (66 S-68 S, 144 E-150 E, Fig. 1) is located in King George V Land, East
52 Antarctica, with an ice tongue extending over 140 km from its grounding line to the tongue front
53 and approximately 30 km wide at the front (Legresy et al., 2004). Much field exploration has
54 been conducted around Mertz and the increasing availability over the last decade of remote
55 sensing, hydrographic surveying, and bathymetric data allows the causes of ice tongue instability
56 to gradually come into focus. From satellite altimetry, a modest elevation change rate of 0.03 m/a
57 (Pritchard et al., 2012) and a freeboard change rate of -0.06 m/a (Wang et al., 2014) were found,

58 which implied that the combined effects of surface accumulation and basal melt were not
59 dramatic for this ice tongue. For the MIT, investigations of tidal effects, surface velocity, rift
60 propagation, and ice front propagation (Berthier et al., 2003; Frezzotti et al., 1998; Legresy et al.,
61 2004; Lescarmonier et al., 2012; Massom et al., 2010, 2015) have been conducted with an
62 objective of detecting underlying factors affecting its stability. Grounding as a potential factor
63 can affect the stability of an ice tongue, ~~as recently pointed out by~~ possibly holding the tongue
64 to delay calving (Massom et al. (2015). However, without highly accurate bathymetric data, it is
65 impossible to carry out such study. Fortunately, In 2010, a new and high resolution bathymetry
66 model, ~~for the seafloor surrounding the Mertz,~~ with a resolution of 100 m was released for the
67 Terra Adelie and George V continental margin (Beaman et al., 2011), and incidentally later used
68 to generate the Bedmap-2 (Fretwell et al., 2013). Such accurate data provides an opportunity for
69 better exploring seafloor shoals and their impacts on the instability of MIT. In this study, we
70 focus on the grounding event of the MIT from 2002 to 2008. A method for grounding event
71 detection is proposed and the grounding of the MIT before calving is investigated. A calving
72 cycle of the MIT caused by grounding on seafloor shoal, Mertz Bank is discussed as well.

73 **2. Data**

74 The primary data used to investigate ~~ice tongue~~ grounding of the MIT in this study are
75 Geoscience Laser Altimeter System (GLAS) data onboard the Ice, Cloud and land Elevation
76 Satellite (ICESat) and the seafloor bathymetry data mentioned above. In this section,
77 ICESat/GLAS and bathymetry data, as well as some preprocessing are introduced.

78 **2.1 ICESat/GLAS**

79 The ICESat is the first spaceborne laser altimetry satellite orbiting the Earth, launched by
80 National Aeronautics and Space Administration (NASA) in 2003 (Zwally et al. 2002) with

81 GLAS as the primary payload onboard. ICESat/GLAS was operated in an orbit of ~600 km and
82 had a geographical coverage from 86°S to 86°N. ICESat/GLAS usually observed in nadir
83 viewing geometry and employed laser pulses of both 532 nm and 1064 nm to measure the
84 distance from the sensor to the ground (Zwally et al. 2002). On the ground, ICESat/GLAS's
85 footprint covered an area of approximately 70 m in diameter, with ~~each~~-adjacent footprints
86 spaced by ~170 m. The horizontal location accuracy of the footprint was about 6 m (Abshire et al.
87 2005). The accuracy and precision of ICESat/GLAS altimetry data were 14 cm and 2 cm
88 respectively (Shuman et al. 2006). ICESat/GLAS usually made two or three campaigns a year
89 from 2003 to the end of 2009, with each campaign lasting for about one month. With billions of
90 laser footprints received by the telescope, 15 different types of data were produced for various
91 scientific applications, named as GLA01, GLA02, ... GLA15. In this study, GLA12 data
92 (elevation data for polar ice sheet) covering the Mertz from release 33 during the interval of 2003
93 to 2009 is used, the spatial distribution of which is shown in Fig. 2.

94 **2.2 Seafloor Topography**

95 Detailed bathymetry maps are fundamentally spatial data for marine science studies
96 (Beaman et al., 2003, 2011) and crucially needed in the data-sparse Antarctic coastal region
97 (Massom et al. 2015). Regionally, around Mertz, a large archive of ship track single-beam and
98 multi-beam bathymetry data from 2000 to 2008 were used to generate a high resolution Digital
99 Elevation Model (DEM), the spatial coverage of which can be found ~~in Fig. 2 of Beaman et al.~~
100 ~~(2011) and bathymetry data coverage over the Mertz region can be found from S-Figs. 1-3(b) and~~
101 ~~3(c)~~. The DEM product was reported as having a vertical accuracy of about 11.5 m (500 m depth)
102 and horizontal accuracy of about 70 m (500 m depth) in the poorest situation (Beaman et al.
103 2011). As can be seen from Fig. 3(b) and Fig. 3(c), there is no bathymetry data under the MIT,

104 which may result in large uncertainty for seafloor interpolation. The oldest bathymetry data
105 collected along the margin of the MIT was at least from 2000 (Beaman et al. 2011). Thus, the
106 boundary of the MIT in 2000 is used to identify bathymetry measurement gaps, as is indicated in
107 Fig. 6. However around the Mertz ice front, for both the east and west flanks, bathymetry data
108 does exist, which provide control points for seafloor interpolation under the tongue. Since the ice
109 front has a width of ~34 km (Wang et al. 2014), the accuracy of seafloor DEM under the MIT
110 varies according to different distance to the control points. Inside of the 2000 boundary of the
111 MIT, the closer to the dash-dotted polygon (Figs. 6 and 7), the better accuracy the seafloor DEM.
112 Outside of that boundary, the quality of the seafloor DEM data is much better because of the
113 high density of single-beam or multi-beam bathymetric measurements.

114 Around Antarctica, seafloor topography data from Bedmap-2 was produced by Fretwell
115 et al. (2013) which adopted the DEM from Beaman et al. (2011). In this study, Bedmap-2
116 seafloor topography data covering Mertz is employed to detect the contact between seafloor and
117 the MIT. Because of inconsistent elevation systems for ICESat/GLAS and seafloor topography
118 data, the Earth Gravitational Model 2008 (EGM08) geoid (Pavlis et al. 2012) with respect to
119 World Geodetic System 1984 (WGS-84) ellipsoid is taken as reference. Since seafloor
120 topography from Bedmap-2 is referenced to the so-called g104c geoid, an elevation
121 transformation is required and can be implemented through Eq. (1).

$$122 \quad E_{sf} = E_{seafloor} + gl04c_{to_wgs84} - EGM2008 \quad (1)$$

123 where E_{sf} and $E_{seafloor}$ is the seafloor topography under EGM08 and g104c respectively,
124 $gl04c_{to_wgs84}$ is the value needed to convert height relative to g104c geoid to that under WGS-84,
125 and $EGM2008$ is the geoid undulation with respect to WGS-84.

126 **3. Methods**

127 | 3.1 Grounding Detection Methods

128 | ICESat/GLAS data has been widely used to determine ice freeboard, or ice thickness,
129 | since its launch in 2003 (Kwok et al., 2007; Wang et al., 2011, 2014; Yi et al., 2011; Zwally et
130 | al., 2002, 2008). ~~To study ice freeboard, draft, and grounding of the MIT through time,~~
131 | ~~ICESat/GLAS GLA12 data from release 33 from 2003 to 2009 are used as mentioned, and the~~
132 | ~~spatial coverage of which can be seen in Fig. 2.~~The methods we designed for grounding
133 | detection of the MIT are now introduced using ICESat/GLAS data. First, assuming a floating ice
134 | tongue, based on freeboard data extracted in different observation dates, the ice draft of the MIT
135 | is inverted. Next, ice bottom elevation is calculated based on the inverted ice draft and the
136 | lowest sea-surface height. Finally, the ice bottom is compared with seafloor bathymetry and ice
137 | grounding is detected. The underlying logic for grounding detection is that if the inverted ice
138 | bottom is lower than seafloor, we can draw a conclusion that the ice tongue is grounded rather
139 | than floating.

140 | The method to extract a freeboard map using ICESat/GLAS from multiple campaigns
141 | over the MIT was described in Wang et al. (2014). Here, we do not revisit it in detail but
142 | introduce it schematically. Four steps are included in freeboard map production for each of the
143 | datasets from November 14, 2002, March 8, 2004, December 27, 2006 and January 31, 2008..

144 | The first step ~~is on~~involves data preprocessing, saturation correction, data quality control,
145 | and tidal correction removal. The magnitude of the ICESat/GLAS waveform can become
146 | saturated because of different gain setting, or ~~the occurrence of cloud~~high reflected natural
147 | surface. Thus the saturated waveforms with *i_satElevCorr* (i.e. an attribute from GLA12 data
148 | record) greater than or equal to 0.50 m are ignored and those with *i_satElevCorr* less than 0.50 m
149 | are corrected ~~by adding the correction back~~following the procedures in (Wang et al. (2012, 2013)).

150 Additionally, measurements with $i_{reflectUC}$ greater than or equal to one are ignored.
151 Furthermore, tidal correction from the TPX07.1 tide model in GLA12 data record is removed to
152 obtain ~~elevation data on estimates of~~ the instantaneous sea surface ~~height~~~~condition~~. Finally,
153 elevation data from ICESat/GLAS related to the WGS-84 ellipsoid and EGM 08 geoid ~~for~~
154 ~~ICESat/GLAS~~ from 2003 to 2009 is prepared-ready for subsequent use.

155 The second step is to derive sea-level-sea-surface height according to each track and to
156 calculate freeboard for each campaign. Because of tidal variations near the MIT, surface
157 elevations of the MIT can vary as well. To derive sea-level-sea-surface height from
158 ICESat/GLAS and provide a reference for freeboard calculation for different campaigns,
159 ICESat/GLAS data over the MIT within a buffer region (with 10 km as buffer radius of MIT
160 boundary in 2007) are selected and sea-level-sea-surface height is determined as the lowest
161 elevation measurement along each track (Wang et al. 2014). Freeboard is then calculated by
162 subtracting the corresponding sea-level-sea-surface height from elevation measurements of the
163 MIT according to different tracks in the same campaign. Thus freeboard data for different
164 campaigns from 2003 to 2009 is obtained.

165 The third step is to relocate footprints using estimated ice velocity. ICESat observed the
166 MIT almost repeatedly along different tracks in different campaigns (Fig. 2). However,
167 observation from only one campaign cannot provide good coverage of the MIT, which drives us
168 to combine all observations from 2003 to 2009 together to produce a freeboard map of MIT. Fig.
169 2 shows the spatial coverage of ICESat/GLAS from 2003 to 2009 over the Mertz, but the
170 geometric relation between tracks is not correct over the MIT because the tongue was fast
171 moving and observed in different years by the ICESat. The region observed in an earlier
172 campaign would move downstream later (Wang et al. 2014). For example, consider ICESat

173 ~~collected~~ data from track T31 on March 22, 2003 and T165 (Fig. 2) on November 1, 2003
 174 respectively. Fig. 2 shows the distance between track T165 and T31, ~~is~~ is ~7.5 km without
 175 ~~considering accounting for ice flow~~ advection between observation dates. However because of
 176 the fast moving ice tongue, the distance of their actual ground tracks on the surface of the MIT
 177 should be ~~a little~~ larger because T165 ~~is~~ was located upstream and observed later. Thus footprints
 178 relocation using ice velocity is critical to obtain accurate geometric relations among different
 179 tracks. The ice velocity data from Rignot et al. (2011) generated from InSAR data from 2006 to
 180 2010 is used to relocate the footprints of ICESat/GLAS. Thus the correct geospatial relations
 181 between observations from different campaigns can be achieved on November 14, 2002, March
 182 8, 2004, December 27, 2006, and January 31, 2008, through Eqs. (2) and (3).

$$183 \quad X = x + \sum_{i=1}^n v_{xi} \Delta t + v_{xm} t_m \quad (2)$$

$$184 \quad Y = y + \sum_{i=1}^n v_{yi} \Delta t + v_{ym} t_m \quad (t_m = t_2 - t_1 - n\Delta t) \quad (3)$$

185 where x and y are locations in the X and Y directions from ICESat measurement directly;

186 X and Y are locations in the X and Y directions after relocation; v_x and v_y are the ice velocities in

187 the X and Y directions respectively; t_1 and t_2 are the start and end times; Δt is the time interval

188 and n indicates the largest integer time steps for time interval between t_1 and t_2 ; t_m is the

189 residual time; In this work, Δt is set as 10 days; v_{xi} and v_{yi} is derived from ice velocity field

190 according to different locations during relocation and may change in different time intervals.

191 The freeboard change with time should be considered as well, but this contribution is
 192 neglected because freeboard comparison from crossing tracks showed a slightly decreasing trend
 193 of -0.06 m/a on average (Wang et al. 2014). The spatial distribution of freeboard data over the
 194 MIT corresponding to November 14, 2002, is shown in Fig. 5(a).

$$195 \quad X = x + \sum_{i=1}^n v_{xi} \Delta t + v_{xm} t_m \quad (2)$$

196
$$Y = y + \sum_{i=1}^n v_{yi} \Delta t + v_{ym} t_m \frac{(t_{ms} - t_{se} - t_{se} - n\Delta t)}{2} \quad (3)$$

197 ~~where x and y are locations in the X and Y directions from ICESat measurement directly;~~
 198 ~~X and Y are locations in the X and Y directions after relocation; v_{xm} and v_{ym} are the ice velocities in~~
 199 ~~the X and Y directions respectively; t_{se} and t_{ms} are the start and end times; Δt is the time interval~~
 200 ~~and n indicates the largest integer time steps for time interval between t_{se} and t_{ms} ; t_{ms} is the~~
 201 ~~residual time; In this work, Δt is set as 10 days; v_{xm} and v_{ym} is derived from ice velocity field~~
 202 ~~according to different locations during relocation and may change in different time intervals.~~

203 The fourth step is to interpolate the freeboard map using the relocated freeboard data from
 204 ~~the third step three. Inverse Distance Weighting, Natural Neighbor, Spline and Kriging are most~~
 205 ~~widely used interpolation techniques (Childs, 2004).~~ Kriging interpolation under spatial analysis
 206 toolbox of ArcGIS is selected in this study to produce freeboard maps of the MIT because it can
 207 provide an optimal interpolation estimate for a given coordinate location by considering the
 208 spatial relationships of a data set. With this method, freeboard maps of the MIT are produced on
 209 November 14, 2002, March 8, 2004, December 27, 2006, and January 31, 2008, ~~because of~~
 210 ~~known ice tongue outlines from Landsat images when the ice tongue outline can be delineated~~
 211 ~~from Landsat images.~~

212 Ice draft is calculated with Eq. (4) assuming hydrostatic equilibrium and using the lowest
 213 sea-surface height ~~(further discussed later in Section 6.2.2)~~ which is extracted ~~as well~~ from
 214 ICESat/GLAS data from all campaigns covering this region, ~~which was~~ 3.35 m under EGM 08
 215 (WGS-84).

216
$$\rho_w D = \rho_i (H_f + D - FAC) \quad (4)$$

217 ~~(4)~~

Formatted: Indent: First line: 0.5"

218 where D is ice draft, i.e. vertical distance from sea surface to bottom of ice; H_f is
219 freeboard, i.e. vertical distance from sea surface to top of snow; ρ_w and ρ_i are densities of
220 ocean water and ice, respectively. In this study, ice and sea water density are taken as 915 kg/m^3
221 and 1024 kg/m^3 , respectively (Wang et al., 2014); FAC is the firm air content, the decrease in
222 thickness (in meters) that occurs when the firm column is compressed to the density of glacier ice,
223 as defined in Holland et al., (2011) and Ligtenberg et al. (2014).

224 The lowest sea surface height -3.35 m is derived by comparing all sea-surface heights
225 derived from different tracks and campaigns from 2003 to 2009. This constant stands for the
226 lowest sea surface height from results around Mertz from 2003 to 2009 and is directly from
227 ICESat/GLAS observation. For time varying sea-surface heights caused by tides, the minimum
228 sea-surface height can allow ice with a given draft to ground to the seafloor. Then, ice bottom
229 elevation is calculated by considering the ice draft and the lowest sea-surface height. To compare
230 the ice bottom with the seafloor, an elevation difference of both is calculated. In this way, a
231 negative value indicates that ice bottom is lower than the seafloor, which corresponds to
232 grounding.

$$233 \rho_w D = \rho_i (H_f + D - FAC) \quad (4)$$

234 ~~where D is ice draft, i.e. vertical distance from sea surface to bottom of ice; H_f is freeboard, i.e.~~
235 ~~vertical distance from sea surface to top of snow; ρ_w and ρ_i are densities of ocean water and ice,~~
236 ~~respectively. In this study, ice and sea water density are taken as 915 kg/m^3 and 1024 kg/m^3 ,~~
237 ~~respectively (Wang et al., 2014); FAC is the firm air content, the decrease in thickness (in meters)~~
238 ~~that occurs when the firm column is compressed to the density of glacier ice, as defined in~~
239 ~~Holland et al., (2011) and Ligtenberg et al. (2014).~~

240 The calculation of firn air content around Mertz is introduced in Section 3.2. In this work,
241 we define the elevation of ~~at~~ the underside (bottom) of the tongue as E_{ice_bottom} and is calculated
242 by Eq. (5).

$$243 \quad E_{ice_bottom} = E_{sea_level} - D \quad (5)$$

244 where E_{ice_bottom} corresponds to elevation of the ice bottom. E_{sea_level} is the lowest sea-surface
245 height among extracted sea-surface height from different tracks and different campaigns, which
246 is -3.35 m.

247 Similarly, the elevation difference of ice tongue bottom and seafloor is defined as E_{dif} ,
248 which can be calculated by Eq. (6).

$$249 \quad E_{dif} = E_{ice_bottom} - E_{sf} \quad (6)$$

250 where E_{difsf} is ~~elevation difference by subtracting~~ the seafloor elevation as defined in Eq. (1)
251 ~~from the ice bottom.~~

252 3.2. Firn Air Content Estimation Method

253 The Antarctic ice sheet is covered by a dry, thick firn layer which represents an
254 intermediate stage between fresh snow and glacial ice, having varying density from Antarctic
255 inland to the coast (~~Van van~~ den Broeke, 2008). The density and depth of the Antarctic firn layer
256 has been modeled (e.g., ~~Van van~~ den Broeke, 2008) using a combination of regional climate
257 model output and a steady-state firn compaction model. However, for ice thickness inversion,
258 Firn Air Content (FAC) is usually used to make the calculation convenient (Rignot and Jacobs.
259 2002) ~~and~~ FAC is defined as the decrease in thickness (in meters) that occurs when the firn
260 column is compressed to the density of glacier ice (Holland et al., 2011). Time-dependent FAC
261 has also been modeled by considering the physical process of the firn layer (e.g., Ligtenberg et al.
262 2014). For the MIT, there are some in-situ measurements of snow thickness available from

Formatted: Indent: First line: 0.5"

Formatted: Indent: First line: 0.5"

263 Massom et al. (2010) who used a snow layer depth of 1 m to derive the thickness of surrounding
264 multi-year, fast sea ice. However on the surface of the MIT, no in-situ measurements of density
265 or depth of firm layer ~~are is~~ available.

266 Because of different density and thickness of the firm layer on top of an ice tongue, it is
267 challenging to simulate the density profile of the MIT without in-situ measurements as control
268 points.— In this study, we use FAC extracted from adjacent seafloor-touching icebergs to
269 investigate the grounding of the MIT rather than FAC from modeling. MIT may be composed of
270 pure ice, water, air, firm or snow that ~~makes ice mass calculation complicated~~ will influence the
271 density of the ice tongue. However, if assuming a pure ice density only to calculate ice mass, the
272 thickness of MIT must be corrected by FAC. FAC correction to ice thickness can be inferred
273 from surrounding icebergs calving from MIT using Eq. (4) when knowing ice draft and
274 freeboard assuming hydrostatic equilibrium.— Thus it is critical to target and use icebergs
275 fulfilling these requirements to solve Eq. (4), such as slightly grounded icebergs above already
276 known seafloor with observed freeboard. From Smith (2011), icebergs can be divided into three
277 categories based on bathymetry and seasonal pack ice distributions: grounded, constrained, and
278 free-drifting icebergs. Without occurrence of pack ice, an iceberg can be free-drifting or
279 grounded. Free-drifting icebergs can move several tens of kilometers per day, such as iceberg A-
280 52 (Smith et al. 2007). Grounded icebergs can be ~~firmly~~ heavily or lightly anchored. Heavily
281 grounded icebergs have firm contact with the seafloor and can be stationary for a long time, such
282 as iceberg B-9B (Massom. 2003). However, slightly grounded icebergs may have little contact
283 with the seafloor and can possibly move slowly under the influence of ocean tide, ocean currents,
284 or winds, but much slower than free-drifting icebergs. The relation of grounded iceberg and to

285 ice drifting velocity is not well-known. However, from slowly drifting or nearly stationary
286 icebergs in open water, we can determine if an iceberg is slightly grounded.

287 Because of the heavily grounded iceberg B-9B to the east of the MIT blocking the
288 drifting of pack ice or icebergs from the east, icebergs located between B-9B and the MIT are
289 most likely generated from the Mertz or Ninnis glaciers. Some icebergs may be slightly
290 grounded as can be detected from remote sensing. We calculate the FAC from these slightly
291 grounded icebergs and later apply it to grounding event detection of the MIT. Around the MIT,
292 the locations of three icebergs ('A', 'B' and 'C') were identified using MODIS and Landsat
293 images in austral summer, 2006 and 2008 and shown in Fig. 4. Fortunately, ICESat/GLAS
294 observed these icebergs on February 23, 2006 (54th day of 2006) and February 18, 2008 (49th
295 day of 2008). This allows us to analyze the behavior of the icebergs three-dimensionally. From
296 Fig. 4a, icebergs 'A', 'B' and 'C' changed position little in about two months (from 28 to 85 day
297 of 2006). Thus we can consider these icebergs slightly grounded. ~~These slightly grounded~~
298 ~~icebergs may plough the seafloor and leave ridges or grooves. In Pine Island Trough, ridges on~~
299 ~~the seafloor have been already found with a range of 1 to 2 m, which was believed to be~~
300 ~~influenced by grounding icebergs drifting with tides (Jakobsson et al. 2011; Woodworth Lynas~~
301 ~~et al. 1991). From this viewpoint, we are confident that under the lowest sea level (lowest tide),~~
302 ~~these iceberg must be grounded, which means that~~ For these slightly grounded icebergs,
303 hydrostatic equilibrium should still apply, so the ice draft inverted from freeboard measurement
304 assuming hydrostatic equilibrium ~~must be greater than or should be~~ equal to water depth. Based
305 on this analysis, we can take water depth as draft to calculate the FAC.

306 Because only 'A' and 'C' were observed by track T1289 of the ICESat/GLAS in 2006,
307 freeboard and water depth from bathymetry for both are used to calculate the FAC (Figs. 3b, 3c,

308 4, 9, and Table 1). However, the icebergs were not stationary, which indicates only some parts
309 were slightly grounded. In this study, only the top two largest freeboard measurements of
310 icebergs ‘A’ and ‘C’ from T1289 in 2006 are employed to calculate the FAC with Eq. (7) with a
311 least-squares method under hydrostatic equilibrium.

$$312 \quad FAC = H_{f_k} + D_k - \frac{\rho_w}{\rho_i} D_k + \varepsilon_k \quad (7)$$

313 where k is used to identify different icebergs ‘A’ or ‘C’, H_f is the top two largest freeboard
314 measurement of each iceberg, D is ice draft which is the same as sea water depth and is taken
315 from seafloor bathymetry directly, ε is a residual for FAC.

316 Table 1 shows the freeboard and seafloor bathymetry under the icebergs in 2006 for FAC
317 calculation and grounding detection of icebergs in 2008 (detailed freeboard values for these
318 icebergs can be seen from [S-Fig. 91](#)). With freeboard and seafloor measurements from icebergs
319 ‘A’ and ‘C’ in 2006 (Table 1), ~~the~~ FAC is calculated as about 4.87 ± 1.31 m. Two icebergs ‘A’
320 and ‘B’ were observed by the same track T1289 of the ICESat/GLAS on February 18, 2008 and
321 thus are used to evaluate the grounding detection by using this FAC. From iceberg trajectories
322 observed by remote sensing (Fig. 4b), we know, iceberg ‘A’ drifted away from its original
323 position. Thus it was not grounded. However, iceberg ‘B’ kept rotating in this period without
324 drifting away, from which we can consider it slightly grounded. Such grounding status
325 determined from remote sensing can also be detected with our method since the elevation
326 difference of ice bottom and seafloor from Table 1 does clearly indicate a slightly grounded
327 iceberg ‘B’ and a floating iceberg ‘A’. Thus, our FAC estimation works well around Mertz.

328 FAC varies across the Antarctica ice sheet, usually decreasing from the interior to the
329 coast. In this section, FAC over Mertz region is derived as 4.87 ± 1.31 m. However other time
330 dependent modeling results from the Mertz region were close to 5-10 meters (Ligtenberg et al.

331 2014). Since there are no in-situ measurements available for verification, further comparison
332 work needs to be conducted. However, this FAC value is derived according to our best
333 knowledge over Mertz and is affected by iceberg status and the maximum freeboard used. Our
334 method is not perfect and there are some shortcomings which should be paid attention to.

335 First, for FAC calculation, icebergs just touching the seafloor should be used in which
336 case the FAC calculated assuming hydrostatic equilibrium is the same as the actual value.
337 However, it is difficult to ascertain whether an iceberg is just touching the seafloor from remote
338 sensing images. The near stationary or slowly rotating iceberg detected with remote sensing may
339 be grounded more severely than those just touching the seafloor, which may result in a calculated
340 FAC theoretically larger than the actual value. Thus, using this FAC result to detect grounding
341 can potentially lead to smaller grounding results. However, once an iceberg or ice tongue is
342 detected as grounded using this FAC content, the result is more convincing.

343 Second, limited observation from ICESat/GLAS may not catch the same and the thickest
344 section of an iceberg. Because ICESat/GLAS observed only several times a year on repeat tracks
345 and icebergs were rotating slowly, the elevation profile in 2006 and 2008 along the same track
346 T1289 may not come from the same ground surface. S-Fig. 1 shows the freeboard of icebergs
347 'A', 'B' and 'C' derived from ICESat/GLAS from 2006 and 2008. By comparing freeboard of
348 iceberg 'A' in 2006 (S-Fig. 1a), and 2008 (S-Fig. 1c), we can find that the maximum freeboard
349 was larger and the freeboard profile was longer in 2006. Comparatively, the smaller freeboard in
350 2008 may be caused by basal melting or observing different portion of iceberg 'A'. Since the
351 larger freeboard measured in 2006 indicates a high possibility of capturing the thickest portion,
352 the freeboard measurement in 2006 is used to invert the FAC. Additionally, iceberg 'A' and 'C'

353 | did show the similar maximum freeboard (Table 1), which is another important reason to select
354 | the measurements in 2006 to invert.

355 | 4. Accuracy of Grounding Detection

356 | The accuracy of E_{dif} is critical to grounding detection of the MIT. From Eq. (1) to (6),
357 | ~~we~~ we find different components of the error sources, such as from sea surface height
358 | determination, ice draft, seafloor bathymetry, and elevation transformation. Meanwhile,
359 | uncertainty of ice draft is primarily determined by that of freeboard and FAC . Furthermore, the
360 | uncertainty of freeboard is influenced by footprint relocation and freeboard changing rates.
361 | Considering all mentioned above, the error source of elevation difference E_{dif} can be
362 | synthesized by Eq. (8):

$$363 \quad \Delta E_{dif} = \Delta E_{sl} + a(\Delta H_f + \Delta E_{re} + \Delta E_{fb_c} + \Delta FAC + \Delta E_{krig}) + \Delta E_{sf} + \Delta E_{trans} \quad (8)$$

364 | where $a = \frac{\rho_i}{\rho_w - \rho_i}$; Δ stands for error of each variable; ΔE_{dif} stands for error of final elevation
365 | difference of ice bottom and seafloor; ΔE_{sl} , ΔH_f , ΔE_{re} , ΔE_{fb_c} , ΔFAC , ΔE_{sf} , ΔE_{krig} , and
366 | ΔE_{trans} stand for errors caused by sea surface height extraction, freeboard extraction, freeboard
367 | relocation, freeboard changing rates, FAC calculation, seafloor bathymetry, kriging interpolation
368 | and elevation system transformation, respectively.

369 | Usually, the influence of elevation system transformation on final elevation difference
370 | can be neglected. Based on the error propagation law, the uncertainty of elevation difference E_{dif}
371 | can be described by Eq. (9):

$$372 \quad \varepsilon E_{dif} = \sqrt{(\varepsilon E_{sl})^2 + a^2[(\varepsilon H_f)^2 + (\varepsilon E_{re})^2 + (\varepsilon E_{fb_c})^2 + (\varepsilon FAC)^2 + (\varepsilon E_{krig})^2] + (\varepsilon E_{sf})^2} \quad (9)$$

373 | where ε indicates the uncertainty of each parameter.

374 4.1 Uncertainty of kriging interpolation

375 Fig. 5a shows the spatial distribution of freeboard data over the MIT used for detecting
376 grounding on November 14, 2002. The spatial difference of ICESat/GLAS between Fig. 2 and
377 Fig. 5 ~~are-is~~ caused by footprint relocation, after which the spatial geometry between different
378 tracks is reasonably correct. In the lower right of the Mertz ice front (Fig. 5a), the crossing track
379 ~~freeboard~~ distance between track T1289 and T165 is about 7 km. In these data gaps, freeboard
380 data used for grounding detection ~~in Section 3.1~~ is interpolated using kriging. Thus, knowing the
381 uncertainty of kriging interpolation is critical to final grounding detection.

382 To investigate interpolation uncertainty of the kriging method, freeboard measurements
383 should be compared with ~~interpolation ones~~ freeboard estimates. Thus, a testing region with
384 freeboard measurements is selected, indicated by a ~~blue~~-dashed blue square in Fig. 5a, about 7
385 km×7 km. A freeboard map is first interpolated with gray dots only (Fig. 5a) using kriging.
386 Then, the freeboard measurements (284 of green dots in Fig. 5a) are compared with interpolation
387 in the square. The spatial distribution and the histogram of freeboard difference derived by
388 subtracting krigged freeboard from freeboard derived from ICESat/GLAS ~~is-are~~ shown in Fig.
389 5b.

390 In this square, the freeboard measurement varies from 31.6 m to 40.0 m with 36.6 m in
391 average. However, the interpolated freeboard varies from 32.9 m to 39.6 m with 35.9 m in
392 average. From the freeboard difference results (Fig. 5b), we find that the ~~interpolation results ed~~
393 freeboards show similar results compared with freeboard derived from ICESat/GLAS. The
394 interpolated freeboard has an accuracy of -0.7 ± 1.8 m. The interpolated freeboard using kriging
395 can reflect the actual freeboard well. ~~Also, the distribution of freeboard difference in Fig. 5b does~~
396 ~~not show obvious geospatial variation trend.~~

397 4.2 Grounding Detection Robustness

398 Since ~~sea-level~~sea surface height is extracted from ICESat/GLAS data track by track, we
399 use ± 0.15 m (Zwally et al. 2002) as the uncertainty of elevation data (εE_{sl}). Also from Wang et
400 al. (2014), we can see the uncertainty of freeboard extraction (εH_f) is ± 0.50 m. From Rignot et al.
401 (2011), the error of ice velocity ranged from 5 m/a to 17 m/a. Assuming that ice velocity varied
402 by 17 m/a (an upper threshold), the relocation error horizontally could reach ± 54 m in an average
403 of three years. Wang et al. (2014) extracted the average slope of the MIT along ice flow direction
404 as 0.00024. However, because of large crevasses on the surface, we use 50 times of this value as
405 a conservative estimate of the average slope. In this way, we can estimate εE_{re} as ± 0.65 m when
406 considering a three-year period. The annual rate of freeboard change from 2003 to 2009 is -0.06
407 m/a (Wang et al. 2014). Therefore, we consider the freeboard stable over this period. However,
408 when combining data from different time periods ~~then,~~ εE_{fb_c} is estimated as about ± 0.18 m if
409 considering ~~three-three-year's~~ time difference. ~~—~~ From Beaman et al. (2011), considering
410 elevation uncertainty at the worst situation when water depth is 500 m, εE_{g104c} is ± 1.5 m. For
411 kriging interpolation, from analysis in Section 4.1, 1.8 m is taken as the uncertainty. Using all
412 these errors above, we calculate the final uncertainty of elevation difference as ± 23 m.

413 From the calculations above, we can say that E_{dif} less than ± 23 m corresponds to a very
414 robust grounding event. However, if ~~the~~ E_{dif} is greater than 23 m, we can-not confirm grounding.
415 E_{dif} in the interval of -23m to 23 m corresponds to slightly grounding or floating. We can also
416 determine different contributions of each separate factor to the overall accuracy. Seafloor
417 bathymetry contributes the largest part and is the dominant factor affecting the accuracy of
418 grounding detection.

419 5. Grounding Detection Results

420 The spatial distribution of elevation difference E_{dif} and outlines of the MIT from 2002 to
421 2008 are shown in Fig. 6. A buffer region with radius of 2 km (region between black and grey
422 lines in Fig. 6) is introduced to investigate grounding potential of the MIT, if it approached there.
423 The elevation difference less than 46 m (twice of elevation difference uncertainty εE_{dif}) both
424 inside and outside of the outline is extracted and the corresponding statistics are shown in Table
425 2. Since the uncertainty to determine a grounding event is about ± 23 m, if some grid points of the
426 MIT have elevation difference E_{dif} less than -23 m, we can conclude that this section of the
427 tongue is almost strongly grounded. The smaller the E_{dif} , the more robust the grounding. ~~From~~
428 ~~the color change patterns of Fig. 6a d, we can see that part of the ice front grounded on the~~
429 ~~shallow Mertz Bank from the end of 2002.~~

430 As illustrated from Table 2, ~~the minimum E_{dif} inside of the MIT in 2002 was 11.9 m and~~
431 ~~the minimum E_{dif} inside of the MIT are-were~~ all less than -23 m ~~after 2002. and T~~the ~~mean and~~
432 ~~minimum of the E_{dif} in the buffer region are-were~~ all less than 0 - 23 m from 2002 to 2008. From
433 this point of view, we conclude that the ice tongue ~~has had~~ grounded on the shallow Mertz Bank
434 at least since November 14, 2002. This result coincides with findings from Massom et al. (2015)
435 who considered that the northwestern extremity of the MIT started to contact with the seafloor
436 shoal in late 2002 to early 2003. Also, it would be difficult for the MIT to approach the buffer
437 region (indicated with yellow to red colors in Fig. 6) as the surrounding Mertz Bank gets
438 shallower and steeper, suggesting substantive grounding potentials. Inside of the MIT, the
439 minimum of elevation difference was just 11.9 m on November 14, 2002, which indicates ~~little~~
440 ~~to no~~slightly grounding. However on March 8, 2004, December 27, 2006, and January 31, 2008,
441 the minimum of elevation difference reached -46.0 m, -52.3 m and -34.8 m respectively, which
442 means strongly significant grounding occurred in some regions. From 2002 to 2008, more

443 regions under the MIT ~~have had~~ E_{dif} less than 46 m, the area of which increased from 8 km² to
444 17 km². Additionally, the mean of E_{dif} under of the tongue for those having E_{dif} less than 46 m
445 gradually ~~decreases-decreased~~ from 28.8 m to 12.3m, according to which we can conclude that
446 the ice front ~~was grounded more significantly-~~ became more firmly grounded as time passed on.
447 Additionally, since the grounding area increased from 8 km² to 17 km² (Table 2) and the mean of
448 E_{dif} decreased from 2002 to 2008, we can say that over the period from 2002 to 2008, the
449 grounding of the northwest flank of the MIT became more widespread.

450 Based on the calculated elevation difference, the grounding outlines of the MIT are
451 delineated for November 14, 2002, March 8, 2004, December 27, 2006 and January 31, 2008,
452 (Fig. 7). For the grounding part of the outline in different years, starting and ending location and
453 perimeter are also extracted, from which we can conclude that the length of the grounding
454 outline of the Mertz Bank ~~is-was~~ only limited to a few kilometers (Table 3). We find that the
455 lower right (northwest) of the MIT was always grounded and that grounding did not occur in
456 other regions (Fig. 6). The shallowest seafloor elevation the ice front touched was ~ -290 m in
457 November 2002. In 2004, 2006, and 2008, the lower right (northwest) of the MIT even
458 approached the contour of -220 m.

459 ~~We find that the lower right (northwest) of the MIT was always grounded and that~~
460 ~~grounding did not occur in other regions (Fig. 6). The shallowest seafloor elevation the ice front~~
461 ~~touched was ~ 290 m in November 2002. In 2004, 2006, and 2008, the lower right (northwest)~~
462 ~~of the MIT even approached the contour of -220 m. Fig. 7 also shows the extension line of west~~
463 ~~flank in November, 2002, from which we can see that if the ice tongue moved along the former~~
464 ~~direction, the ice flow would be seriously blocked when approaching the Mertz Bank. The~~
465 ~~shallowest region of the Mertz Bank has an elevation of about -140 m and the MIT would have~~

466 ~~needed to climb the 140 m obstacle to cross it. The shallow Mertz Bank would have caused~~
467 ~~grounding during the climbing. This special feature of seafloor shoal facing the MIT can further~~
468 ~~explain why the ice velocity differed along the east and west flanks of the MIT before calving~~
469 ~~and why the ice tongue moved clockwise to the east, as pointed out by Massom et al. (2015).~~
470 ~~However, because of sparsely distributed bathymetry data (point measurements) in Mertz region~~
471 ~~used in Massom et al. (2015), this effect could not be easily seen. Here, from our grounding~~
472 ~~detection results and surrounding high-accuracy bathymetry data, this effect is more clearly~~
473 ~~observed.~~

474 **6. Discussion**

475 **6.1 Area Changing Rate and ~70-year Calving Cycle of MIT**

476 Using Landsat TM/ETM+ images from 1989 to 2013, outlines of the MIT are extracted
477 manually. Assuming a fixed grounding line position ~~over this period~~, the area of the MIT over
478 this period is calculated. Using these data, from 1989 to 2007, an increasing area rate of the MIT
479 is shown (from 5453 km² to 6126 km²) in Fig. 8. However, the area of the MIT was almost
480 constant from 2007 to 2010, before calving. The largest area of the MIT was 6113 km² closest to
481 the calving event in 2010. After the calving, the area decreased to 3617 km² in November 2010.

482 The rate of area change for the MIT from 1989 to 2007 is also obtained using a least-
483 squares method, corresponding to 35.3 km²/a. However, after the calving a slight higher area-
484 increasing trend of 36.9 km²/a, is found (Fig. 8). On average, the area-increasing rate of the MIT
485 was 36 km²/a.

486 The surface behavior such as ice flow direction changes and middle rift changes caused
487 by grounding was analyzed by Massom et al. (2015). In the history of the MIT, one or two large
488 calving events were suspected to have happened between 1912 and 1956 (Frezzotti et al., 1998).

489 ~~Based on the interactions between the MIT and Mertz Bank suggested by our observations and~~
490 ~~described below, and we consider it is likely that only one large calving event occurred between~~
491 ~~1912 and 1956, to be only once because of the influence of the shallow Mertz Bank.~~ When the
492 ice tongue touched the bank, the bank started to affect the stability of the tongue by bending the
493 ice tongue clockwise to the east, as can be seen from velocity changes from Massom et al. (2015).
494 With continuous ~~momentum advection of ice~~ and flux input from upstream, a large rift from the
495 west flank of the tongue would ultimately have to occur and could potentially calve the tongue.
496 A sudden length shortening of the tongue can be caused by such ice tongue calving as indeed had
497 happened in February, 2010. We also consider that even without a sudden collision of iceberg B-
498 9B in 2010, the ice tongue would eventually calve because of existence of the shallow Mertz
499 Bank.

500 If we take 6127 km^2 as the maximum area of the MIT, assuming a constant area-changing
501 rate of about $36.9 \text{ km}^2/\text{a}$ after 2010, it will take about 68 years to calve again. When assuming an
502 area changing rate of about $35.3 \text{ km}^2/\text{a}$ as before 2010, it will take a little longer, about 71 years.
503 Therefore, without considering accidental event such as collision with other large icebergs, the
504 MIT is predicted to calve again in ~ 70 years. Because of the continuous ~~advection of ice from~~
505 ~~upstream and the fixed location of the shallow Mertz Bank ice flow upstream, the special location~~
506 ~~and relatively lower depth of the Mertz Bank,~~ the calving is likely repeatable and a cycle
507 therefore exists.

508 After the MIT calved in February, 2010, Mertz polynya size, sea-ice production, sea-ice
509 coverage and high-salinity shelf water formation changed. ~~—~~ A sea-ice production decrease of
510 about 14-20% was found by Tamura et al. (2012) using satellite data and high-salinity shelf
511 water export was reported to reduce up to 23% using a state-of-the-art ice-ocean model

512 (Kusahara et al. 2010). Recently, Campagne et al. (2015) pointed out a ~70-year cycle of surface
513 ocean condition and high-salinity shelf water production around Mertz through analyzing
514 reconstructed sea ice and ocean data over the last 250 years. They also mentioned that this cycle
515 was closely related to presence and activity of the Mertz polynya. However, the reason for this
516 cycle was not fully understood.

517 From these findings addressed above and MIT calving cycle we found, our explanation is
518 that the calving cycle of the MIT leads to the ~70-year cycle of surface ocean condition and
519 high-salinity shelf water production around Mertz. Different length of the MIT can prevent sea
520 ice drifting from east side differently. A long MIT contributes to maintain a large polynya
521 because more sea ice formed on the east side could not drift to the west side. With the effect of
522 katabatic wind, sea ice produced from the west side is blown seaward which maintains polynya
523 size and stable sea ice production. Calving decreases the length of the MIT suddenly. Then, a
524 short ice tongue reduces the size of Mertz Polynya formed by Antarctic katabatic winds,
525 resulting in lower sea-ice production and further lessens high-salinity shelf water production.
526 Therefore, the cycle of ocean conditions around Mertz found by Campagne et al. (2015) is likely
527 dominated by the calving of the MIT. Additionally, the 70 year cycles of MIT calving coincides
528 with surface ocean condition change around Mertz well, which makes the explanation much more
529 compelling.

530 **~~6.2 Key issues influencing grounding detection~~**

531 ~~Several issues on grounding detection require further clarification, such as sea surface~~
532 ~~height, FAC value and accuracy of seafloor DEM. In this section, their influences on final~~
533 ~~grounding detection results are more deeply discussed.~~

534 **~~6.2.1 The Lowest Sea Level Extraction~~**

535 ~~In Section 3.1, the lowest sea level 3.35 m is derived by comparing all sea surface~~
536 ~~heights derived from different tracks and campaigns from 2003 to 2009. This constant stands for~~
537 ~~the lowest sea level from results around Mertz from 2003 to 2009 and is directly from~~
538 ~~ICESat/GLAS observation. However, because of limited observations in each year,~~
539 ~~ICESat/GLAS may not catch the lowest one. Sea level lower than 3.35 m may exist over Mertz~~
540 ~~region which would make the grounding results more severe with occurrence of more negative~~
541 ~~values in Fig. 6.~~

542 **6.2.2 Firn Air Content Calculation**

Formatted: Indent: First line: 0.5"

543 ~~FAC varies across the Antarctica ice sheet, usually decreasing from the interior to the~~
544 ~~coast. In Section 3.2, FAC over Mertz region is derived as 4.87 ± 1.31 m. However other time~~
545 ~~dependent modeling results from the Mertz region were closed to 5–10 meters (Ligtenberg et al.~~
546 ~~2014). Since there are no in situ measurements available for verification, further comparison~~
547 ~~work needs to be conducted. However, this FAC value is derived according to our best~~
548 ~~knowledge over Mertz and is affected by iceberg status (using our approach) and the maximum~~
549 ~~freeboard used.~~

550 ~~First, for FAC calculation, icebergs just touching the seafloor should be used in which~~
551 ~~ease the FAC calculated assuming hydrostatic equilibrium is the same as the actual value.~~
552 ~~However, it is difficult to ascertain whether an iceberg is just touching the seafloor from remote~~
553 ~~sensing images. The near stationary or slowly rotating iceberg detected with remote sensing~~
554 ~~should be grounded more severely than just touching the seafloor, which may result in a~~
555 ~~calculated FAC theoretically larger than the actual value. Thus, using this FAC result to detect~~
556 ~~grounding can potentially lead to smaller grounding results. However, once an iceberg or ice~~
557 ~~tongue is detected as grounded, the result is more convincing.~~

558 Second, because ICESat/GLAS observed only several times a year on repeat tracks and
559 icebergs was rotating slowly, the elevation profile in 2006 and 2008 along the same track T1289
560 may not come from the same ground surface. Fig. 9 shows the freeboard over iceberg 'A', 'B'
561 and 'C' derived from ICESat/GLAS from 2006 and 2008. By comparing freeboard of iceberg 'A'
562 in 2006 (Fig. 9a), and 2008 (Fig. 9c), we can find that the maximum freeboard was larger and the
563 freeboard profile was longer in 2006. Comparatively, the smaller freeboard in 2008 may be
564 caused by ice basal melting or observing different portion of iceberg 'A'. Since the larger
565 freeboard measured in 2006 indicates a high possibility of capturing the thickest portion, the
566 freeboard measurement in 2006 is used to invert the FAC. Additionally, iceberg 'A' and 'C' did
567 show the similar maximum freeboard (Table 1), which is another important reason to select the
568 measurement in 2006 to invert.

569 **6.2.3 Seafloor DEM**

570 High-accuracy seafloor elevation is critical to the final success of grounding detection. As
571 can be seen from S Fig.1, there is no bathymetry data under the MIT, which may result in large
572 uncertainty for seafloor interpolation. The oldest bathymetry data collected along the margin of
573 the MIT was at least from 2000 (Beaman et al. 2011). Thus, the boundary of the MIT in 2000 is
574 used to identify bathymetry measurement gaps, as is indicated in Fig. 6. But around the Mertz ice
575 front, for both the east and west flanks, bathymetry data does exist, which provides control points
576 for seafloor interpolation under the tongue. Since the ice front has a width of ~34 km (Wang et al.
577 2014), the accuracy of seafloor DEM under the MIT varies according to different distances to the
578 control points. Inside of the MIT boundary of 2000, the closer to the dash dotted polygon (Figs.
579 6 and 7), the better the accuracy the seafloor DEM. Outside of that boundary, the quality of the

580 ~~seafloor DEM data is much better because of the high density of single beam or multi beam~~
581 ~~bathymetry measurements.~~

582 ~~However, from Beaman et al. (2011), no uncertainty on the seafloor DEM was~~
583 ~~systematically provided. Instead, only the poorest accuracy of single or multi beam bathymetric~~
584 ~~measurements was available. Since no new bathymetry data is publicly available in this region, it~~
585 ~~is not possible to conduct further work on evaluation of the seafloor bathymetry and interpolation~~
586 ~~error from kriging using bathymetry data is difficult to assess. Thus, the accuracy under poorest~~
587 ~~situation for bathymetry data is used, the same as used in Beaman et al. (2011).~~

588 High accuracy seafloor elevation is critical to the final success of grounding detection.

589 Since Beaman et al. (2011) provided the most accurate seafloor DEM over Mertz according to
590 our best knowledge, seafloor DEM inside of dash-dotted polygon (Fig. 7) is kept and the
591 grounding detection is conducted there (Fig. 6) as well. Additionally, the ice tongue never
592 stopped flowing further into the ocean, where the bathymetry measurements density is good.
593 From results shown in Fig. 6 all grounding sections of MIT boundary are located outside of the
594 2000 boundary. Thus the analysis of grounding detection near ice front in 2002, 2004, 2006, and
595 2008 is convincing. Inside of the 2000 boundary, most of the grounding detection results are
596 above 100 m, indicating a floating status of the corresponding ice. Only abnormal seafloor
597 features higher than this seafloor DEM by about 100 m can result in wide grounding inside.

598 ~~Additionally, from surface features of the MIT from Landsat TM/ETM+ images, no abrupt~~
599 ~~sunlight shadow related to grounding is detected from 1989 to 2010 near the front, which~~
600 ~~indicates that the judgment of floating ice tongue inside of the 2000 boundary from Fig. 6 is~~
601 ~~correct.~~—Actually, no matter whether the MIT inside of the 2000 boundary was grounded or not,

602 gradual grounding on the shallow Mertz Bank of the MIT since late 2002 is a fact, which is
603 direct evidence for us to infer the primary cause of the instability of the MIT.

604 **6.3 Influence of Mertz Bank on MIT**

605 Fig. 7 also shows the extension line of west flank in November, 2002, from which we can
606 see that if the ice tongue MIT moved advected along the former direction, the ice flow would be
607 seriously blocked when approaching the Mertz Bank. The shallowest region of the Mertz Bank
608 has an elevation of about -140 m and the MIT would have needed to climb the 140 m obstacle to
609 cross it. The shallow Mertz Bank would have caused strongly grounding during the climbing.
610 This special feature of seafloor shoal facing the MIT can further explain why the ice velocity
611 differed along the east and west flanks of the MIT before calving and why the ice tongue was
612 deflected moved clockwise to the east, as pointed out by Massom et al. (2015). However,
613 because of sparsely-distributed bathymetry data (point measurements) in Mertz region used in
614 Massom et al. (2015), this effect could not be easily seen. Here, from our grounding detection
615 results and surrounding high-accuracy bathymetry data, this effect is more clearly observed.

616

617 **7. Conclusion**

618 In this study, a method of FAC calculation from seafloor-touching icebergs around Mertz
619 region is presented as an important element of understanding MIT grounding. The FAC around
620 the Mertz is about 4.87 ± 1.31 m. This FAC is used to calculate ice draft based on sea-level sea
621 surface height and freeboard extracted from ICESat/GLAS and appears to is verified working
622 well. A method to extract grounding sections of the MIT is described based on comparing
623 inverted ice draft assuming hydrostatic equilibrium with seafloor bathymetry. The final
624 grounding results explain the surface behavior of the MIT. Previous work by Massom et al.

Formatted: Font: Bold

Formatted: Indent: First line: 0"

Formatted: Font: Bold

625 (2015) has also provided some evidence for seafloor interaction, in showing that the MIT front
626 had an approximate 280 m draft with the nearby seafloor as shallow as 285 m, suggesting the
627 possibility of grounding. In our work, we have provided ample detailed bathymetry and ice draft
628 calculations. Specifically, ice bottom elevation is inverted using ICESat/GLAS data and
629 compared with seafloor bathymetry during 2002, 2004, 2006, and 2008. From those calculations
630 we show conclusively that the MIT was indeed grounded along a specific portion of its
631 northwest flank over a limited region. We also point out that even without collision by iceberg
632 B-9B in early 2010 the ice tongue would eventually have calved because of ~~momentum and flux~~
633 ~~in~~ice advection from the upstream and glacier flow being increasingly opposed by a reaction
634 force from the seafloor shoal of the Mertz Bank.

635 From remote sensing images we are able to quantify the rate of increase of area of the
636 MIT before and after the 2010 calving. While the area-increasing trend of the MIT after calving
637 is slightly larger than before, we use the averaged rate to estimate a timescale required for the
638 MIT to re-advance to the area of the shoaling bathymetry from its retreated, calved position. Our
639 estimate is ~70-years, which is remarkably consistent with Campagne et al. (2015) who found a
640 similar period of sea surface changes using seafloor sediment data. A novel point we bring out in
641 our study is that it is the shoaling of the seafloor combined with the rate of advance of the MIT
642 that leads to the 70-year repeat cycle. Also the calving cycle of the MIT explains the observed
643 cycle of sea surface conditions change well, which indicates the calving of the MIT is the
644 dominant factor for sea-surface condition change. Understanding the mechanism underlying the
645 periodicity of MIT calving is important as the presence or absence of the MIT has a profound
646 impact on sea ice and hence of bottom water formation in the local region.

647 **Acknowledgements**

648 This research was supported by Fundamental Research Fund for the Central University,
649 the Center for Global Sea Level Change (CSLC) of NYU Abu Dhabi (Grant: G1204), the Open
650 Fund of State Key Laboratory of Remote Sensing Science (Grant: OFSLRSS201414), and the
651 China Postdoctoral Science Foundation (Grant: 2012M520185, 2013T60077). We are grateful to
652 the Chinese Arctic and Antarctic Administration, the European Space Agency for free data
653 supply under project C1F.18243, the National Snow and Ice Data Center (NSIDC) for the
654 availability of the ICESat/GLAS data (<http://nsidc.org/data/order/icesat-glas-subsetter>) and
655 MODIS image archive over the Mertz glacier ([http://nsidc.org/cgi-](http://nsidc.org/cgi-bin/modis_iceshelf_archive.pl)
656 [bin/modis_iceshelf_archive.pl](http://nsidc.org/cgi-bin/modis_iceshelf_archive.pl)), British Antarctica Survey for providing Bedmap-2 seafloor
657 topography data (<https://secure.antarctica.ac.uk/data/bedmap2/>), the National Geospatial-
658 Intelligence Agency for publicly released EGM2008 GIS data ([http://earth-](http://earth-info.nga.mil/GandG/wgs84/gravitymod/egm2008/egm08_gis.html)
659 [info.nga.mil/GandG/wgs84/gravitymod/egm2008/egm08_gis.html](http://earth-info.nga.mil/GandG/wgs84/gravitymod/egm2008/egm08_gis.html)), and the USGS for Landsat
660 data (<http://glovis.usgs.gov/>). Fruitful discussions with M. Depoorter, P. Morin, T. Scambos and
661 R. Warner, and constructive suggestions from Editor Andreas Vieli and two anonymous
662 reviewers are acknowledged.

663 References

- 664 1. Abshire, J. B., Sun, X., Riris, H., Sirota, J. M., McGarry, J. F., Palm, S. ... & Liiva, P.
665 (2005). Geoscience laser altimeter system (GLAS) on the ICESat mission: on - orbit
666 measurement performance. *Geophysical Research Letters*, 32(21).
- 667 1-2 Beaman, R. J., & Harris, P. T. (2003). Seafloor morphology and acoustic facies of the
668 George V Land shelf. *Deep Sea Research Part II: Topical Studies in Oceanography*,
669 50(8), 1343-1355.

Formatted: Font: Italic

- 670 | ~~2.3~~ Beaman, R. J., O'Brien, P. E., Post, A. L., & De Santis, L. (2011). A new high-resolution
671 | bathymetry model for the Terre Adélie and George V continental margin, East Antarctica.
672 | *Antarctic Science*, 23(01), 95-103.
- 673 | ~~3.4~~ Berthier, E., Raup, B., & Scambos, T. (2003). New velocity map and mass-balance
674 | estimate of Mertz Glacier, East Antarctica, derived from Landsat sequential imagery.
675 | *Journal of Glaciology*, 49(167), 503-511.
- 676 | ~~4. Ballantyne, J., 2002. A multidecadal study of the number of Antarctic icebergs using~~
677 | ~~scatterometer data. Brigham Young University online report:~~
678 | ~~(<http://www.sep.byu.edu/data/iceberg/IcebergReport.pdf>)~~.
- 679 | 5. Campagne, P., Crosta, X., Houssais, M. N., Swingedouw, D., Schmidt, S., Martin, A., ...
680 | & Massé G. (2015). Glacial ice and atmospheric forcing on the Mertz Glacier Polynya
681 | over the past 250 years. *Nature Communications*, 6.
- 682 | ~~6. Childs, C. (2004). Interpolating surfaces in ArcGIS spatial analyst. ArcUser, July-~~
683 | ~~September, 3235.~~
- 684 | ~~7.6~~ Depoorter, M. A., Bamber, J. L., Griggs, J. A., Lenaerts, J. T. M., Ligteneberg, S. R. M.,
685 | van den Broeke, M. R., & Moholdt, G. (2013). Calving fluxes and basal melt rates of
686 | Antarctic ice shelves. *Nature*, 502(7469), 89-92.
- 687 | ~~8.7~~ Domack, E., Duran, D., Leventer, A., Ishman, S., Doane, S., McCallum, S., ... & Prentice,
688 | M. (2005). Stability of the Larsen B ice shelf on the Antarctic Peninsula during the
689 | Holocene epoch. *Nature*, 436(7051), 681-685.
- 690 | ~~9.8~~ Fretwell, P., Pritchard, H. D., Vaughan, D. G., Bamber, J. L., Barrand, N. E., Bell, R., ...
691 | & Fujita, S. (2013). Bedmap2: improved ice bed, surface and thickness datasets for
692 | Antarctica. *Cryosphere*, 7(1).

- 693 | ~~10.9.~~ Frezzotti, M., Cimbelli, A., & Ferrigno, J. G. (1998). Ice-front change and iceberg
694 | behaviour along Oates and George V Coasts, Antarctica, 1912-96. *Annals of Glaciology*,
695 | 27, 643-650.
- 696 | ~~11. Fricker, H. A., Young, N. W., Allison, I., & Coleman, R. (2002). Iceberg calving from~~
697 | ~~the Amery ice shelf, East Antarctica. *Annals of Glaciology*, 34(1), 241-246.~~
- 698 | ~~12. Griggs, J. A., & Bamber, J. L. (2011). Antarctic ice shelf thickness from satellite radar~~
699 | ~~altimetry. *Journal of Glaciology*, 57(203), 485-498.~~
- 700 | ~~13.10.~~ Holland, P. R., Corr, H. F., Pritchard, H. D., Vaughan, D. G., Arthern, R. J.,
701 | Jenkins, A., & Tedesco, M. (2011). The air content of Larsen ice shelf. *Geophysical*
702 | *Research Letters*, 38(10).
- 703 | ~~14. Jakobsson, M., Anderson, J. B., Nitsche, F. O., Dowdeswell, J. A., Gyllencreutz, R.,~~
704 | ~~Kirchner, N., ... & Majewski, W. (2011). Geological record of ice shelf break-up and~~
705 | ~~grounding-line retreat, Pine Island Bay, West Antarctica. *Geology*, 39(7), 691-694.~~
- 706 | ~~15. Jenkins, A., Dutrioux, P., Jacobs, S. S., McPhail, S. D., Perrett, J. R., Webb, A. T., &~~
707 | ~~White, D. (2010). Observations beneath Pine Island Glacier in West Antarctica and~~
708 | ~~implications for its retreat. *Nature Geoscience*, 3(7), 468-472.~~
- 709 | ~~16. Joughin, I., & Alley, R. B. (2011). Stability of the West Antarctic ice sheet in a warming~~
710 | ~~world. *Nature Geoscience*, 4(8), 506-513.~~
- 711 | ~~17.11.~~ Kusahara, K., Hasumi, H. & Williams, G. D. (2011), Impact of the Mertz Glacier
712 | Tongue calving on dense water formation and export. *Nature communications*, 2, 159.
- 713 | ~~18. Kern, S., & Spreen, G. (2015), Uncertainties in Antarctic sea ice thickness retrieval from~~
714 | ~~ICESat. *Annals of Glaciology*, 56(69), 107.~~

715 | ~~19~~12. Kwok, R. Cunningham, G. F., Zwally, H. J., & Yi, D. (2007). Ice, Cloud, and
716 | land Elevation Satellite (ICESat) over Arctic sea ice: retrieval of freeboard. *Journal of*
717 | *Geophysical Research*, 112, C12013, doi:10.1029/2006JC003978.

718 | ~~20~~13. Legresy, B., Wendt, A., Tabacco, I. E., Remy, F., & Dietrich, R. (2004). Influence
719 | of tides and tidal current on Mertz Glacier, Antarctica. *Journal of Glaciology*, 50(170),
720 | 427-435.

721 | ~~21~~14. Legresy, B., N. Young, L. Lescarmonier, R. Coleman, R. Massom, B. Giles, A.
722 | Fraser, R. Warener, B. Galton-Fenzi, L. Testut, M. Houssais and G. Masse (2010),
723 | CRAC!!! in the Mertz Glacier, Antarctica.
724 | [http://www.antarctica.gov.au/__data/assets/pdf_file/0004/22549/ml_402353967939815_](http://www.antarctica.gov.au/__data/assets/pdf_file/0004/22549/ml_402353967939815_mertz_final_100226.pdf)
725 | [mertz_final_100226.pdf](http://www.antarctica.gov.au/__data/assets/pdf_file/0004/22549/ml_402353967939815_mertz_final_100226.pdf)

726 | ~~22~~15. Lescarmonier, L., Legrésy, B., Coleman, R., Perosanz, F., Mayet, C., & Testut, L.
727 | (2012). Vibrations of Mertz glacier ice tongue, East Antarctica. *Journal of Glaciology*,
728 | 58(210), 665-676.

729 | ~~23. Ligtenberg, S. R. M., Heilsen, M. M., & van de Broeke, M. R. (2011). An improved~~
730 | ~~semi empirical model for the densification of Antarctic firn. *The Cryosphere*, 5(4), 809-~~
731 | ~~819.~~

732 | ~~24~~16. Ligtenberg, S., Kuipers Munneke, P., & Van Den Broeke, M. R. (2014). Present
733 | and future variations in Antarctic firn air content. *The Cryosphere*, 8(5), 1711-1723.

734 | ~~25~~17. Massom, R. A. (2003). Recent iceberg calving events in the Ninnis Glacier region,
735 | East Antarctica. *Antarctic Science*, 15(02), 303-313.

736 | ~~26~~18. Massom, R. A., Giles, A. B., Fricker, H. A., Warner, R. C., Legrésy, B., Hyland,
737 | G., Young, N., & Fraser, A. D. (2010). Examining the interaction between multi-year

738 landfast sea ice and the Mertz Glacier Tongue, East Antarctica: Another factor in ice
739 sheet stability? *Journal of Geophysical Research*, 115, C12027,
740 doi:10.1029/2009JC006083.

741 ~~27~~¹⁹. Massom, R. A., Giles, A. B., Warner, R. C., Fricker, H. A., Legrésy, B., Hyland,
742 G., ... & Young, N. (2015). External influences on the Mertz Glacier Tongue (East
743 Antarctica) in the decade leading up to its calving in 2010. *Journal of Geophysical*
744 *Research: Earth Surface*, 120(3), 490-506.

745 ~~28~~²⁰. Pavlis, N. K., Holmes S. A., Kenyon, S. C., & Factor, J. K. (2012). The
746 development and evaluation of the Earth Gravitational Model 2008 (EGM2008), *Journal*
747 *of Geophysical Research*. 117, B04406, doi:10.1029/2011JB008916.

748 ~~29~~. Porter Smith, R. (2003). Bathymetry of the George Vth Land shelf and slope. *Deep Sea*
749 *Research Part II: Topical Studies in Oceanography*, 50(8), 1337-1341.

750 ~~30~~²¹. Pritchard, H. D., Ligtenberg, S. R. M., Fricker, H. A., Vaughan, D. G., Van den
751 Broeke, M. R., & Padman, L. (2012). Antarctic ice-sheet loss driven by basal melting of
752 ice shelves. *Nature*, 484(7395), 502-505.

753 ~~31~~²². Rignot, E., Mouginot, J. & Scheuchl, B. (2011), Ice flow of the Antarctic ice sheet.
754 *Science*, 333(6048), 1427-1430.

755 ~~32~~²³. Rignot, E., & Jacobs, S. S. (2002). Rapid bottom melting widespread near
756 Antarctic ice sheet grounding lines. *Science*, 296(5575), 2020-2023.

757 ~~33~~²⁴. Scambos, T. Hulbe, A., C. & Fahnestock, M. A. (2003). Climate-induced ice shelf
758 disintegration in the Antarctic Peninsula. *Antarctic Research Series*, 79, 79-92.

- 759 | ~~34-25.~~ Scambos, T. Hulbe, A., C. Fahnestock, M. A. & Bohlander, J. (2000). The link
760 | between climate warming and breakup of ice shelves in the Antarctic Peninsula. *Journal*
761 | *of Glaciology*, 46(154), 516-530.
- 762 | ~~35-26.~~ Shepherd, A., Wingham, D., Payne, T., & Skvarca, P. (2003). Larsen Ice Shelf
763 | has progressively thinned. *Science*, 302(5646), 856-859.
- 764 | 27. Shuman, C. A., Zwally, H. J., Schutz, B. E., Brenner, A. C., DiMarzio, J. P., Suchdeo, V.
765 | P., & Fricker, H. A. (2006). ICESat Antarctic elevation data: Preliminary precision and
766 | accuracy assessment. *Geophysical Research Letters*, 33(7).
- 767 | ~~36-28.~~ Smith, K. L., Robison, B. H., Helly, J. J., Kaufmann, R. S., Ruhl, H. A., Shaw, T.
768 | J., ... & Vernet, M. (2007). Free-drifting icebergs: hot spots of chemical and biological
769 | enrichment in the Weddell Sea. *Science*, 317(5837), 478-482.
- 770 | ~~37-29.~~ Smith, K. L. (2011). Free-drifting icebergs in the Southern Ocean: an overview.
771 | *Deep Sea Research Part II: Topical Studies in Oceanography*, 58(11), 1277-1284.
- 772 | ~~38-30.~~ Tamura, T., Williams, G. D., Fraser, A. D. & Ohshima, K. I. (2012). Potential
773 | regime shift in decreased sea ice production after the Mertz Glacier calving, *Nature*
774 | *communications*, 3, 826.
- 775 | ~~39. Tehernia, P. A. U. L., & Jeannin, P. F. (1984). Circulation in Antaretic waters as revealed~~
776 | ~~by iceberg tracks 1972–1983. *Polar Rec*, 22(138), 263–269.~~
- 777 | ~~40. Van de Berg, W. J., Van den Broeke, M. R., Reijmer, C. H., & Van Meijgaard, E. (2005).~~
778 | ~~Characteristics of the Antaretic surface mass balance, 1958–2002, using a regional~~
779 | ~~atmospheric climate model. *Annals of glaciology*, 41(1), 97–104.~~
- 780 | ~~41. Van de Berg, W. J., Van den Broeke, M. R., Reijmer, C. H., & Van Meijgaard, E. (2006).~~
781 | ~~Reassessment of the Antaretic surface mass balance using calibrated output of a regional~~

Formatted: Font: Italic

782 | ~~atmospheric climate model. *Journal of Geophysical Research: Atmospheres* (1984–2012),~~
783 | ~~11(D11).~~

784 | 42-31. ____ Van den Broeke, M. (2008). Depth and density of the Antarctic firn layer. *Arctic,*
785 | *Antarctic, and Alpine Research*, 40(2), 432-438.

786 | 43-32. ____ Wang, X.W., Cheng, X., Gong, P., Huang, H. B., Li Z., & Li, X. W. (2011). Earth
787 | Science Applications of ICESat/GLAS: a Review. *International Journal of Remote*
788 | *Sensing*, 32, 23, 8837-8864, doi: 10.1080/01431161.2010.547533

789 | 44-33. ____ Wang, X.W., Cheng, X., Gong, P., Shum, C. K., Holland, D.M., & Li, X.W.
790 | (2014). Freeboard and mass extraction of the disintegrated Mertz Ice Tongue with remote
791 | sensing and altimetry data. *Remote Sensing of Environment*, 144, 1-10.

792 | 45-34. ____ Wang, X.W. (2014). Mertz ice tongue evolutions from satellite observed data,
793 | Postdoctoral Research Report, College of Global Change and Earth System Science,
794 | Beijing Normal University, China. doi: 10.13140/2.1.1006.1603

795 | 46-35. ____ Wang, X., Cheng, X., Li, Z., Huang, H., Niu, Z., Li, X., & Gong, P. (2012). Lake
796 | water footprint identification from time-series ICESat/GLAS data. *Geoscience and*
797 | *Remote Sensing Letters, IEEE*, 9(3), 333-337.

798 | 47-36. ____ Wang, X., Gong, P., Zhao, Y., Xu, Y., Cheng, X., Niu, Z., ... & Li, X. (2013).
799 | Water-level changes in China's large lakes determined from ICESat/GLAS data. *Remote*
800 | *Sensing of Environment*, 132, 131-144.

801 | ~~48. Woodworth Lynas, C. M. T., Josenhans, H. W., Barrie, J. V., Lewis, C. F. M., & Parrott,~~
802 | ~~D. R. (1991). The physical processes of seabed disturbance during iceberg grounding and~~
803 | ~~scouring. *Continental Shelf Research*, 11(8), 939-961.~~

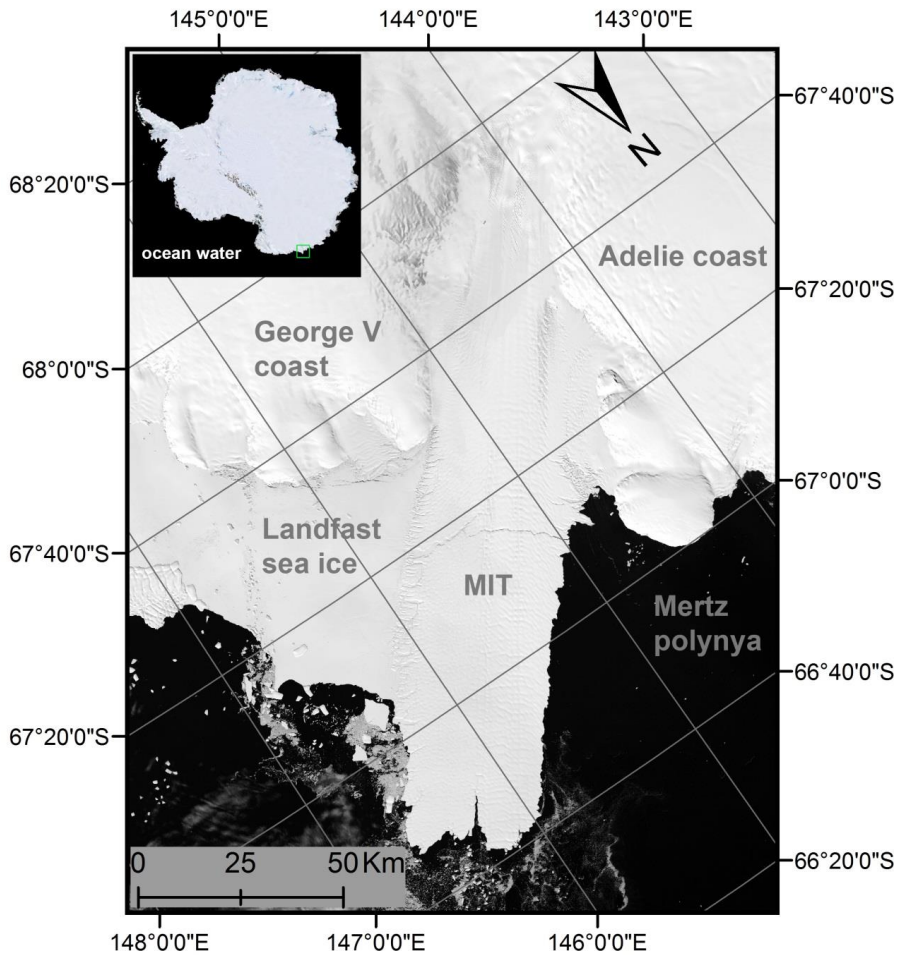
804 | ~~49,37.~~ Yi, D., Zwally, H.J., & Robbins, J. (2011). ICESat observations of seasonal and
805 | interannual variations of sea-ice freeboard and estimated thickness in the Weddell Sea,
806 | Antarctica (2003-2009). *Annals of Glaciology*, 52(57), 43-51.

807 | ~~50,38.~~ Zwally, H. J., Schutz, B., Abdalati, W., Abshire, J., Bentley, C., Brenner, A.,
808 | Buftona, J., Deziof, J., Hancocka, D., Hardinga, D., Herringg, T., Minsterh, B.,
809 | Quinng, K., Palmi, S., Spinhirnea, J., & Thomasj, R. (2002). ICESat's laser
810 | measurements of polar ice, atmosphere, ocean, and land. *Journal of Geodynamics*, 34,
811 | 405-445.

812 | ~~51,39.~~ Zwally, H. J., Yi, D., Kwok, R., & Zhao, Y. (2008). ICESat measurements of sea
813 | ice freeboard and estimates of sea ice thickness in the Weddell Sea. *Journal of*
814 | *Geophysical Research*, 113, C02S15, doi:10.1029/2007JC004284.

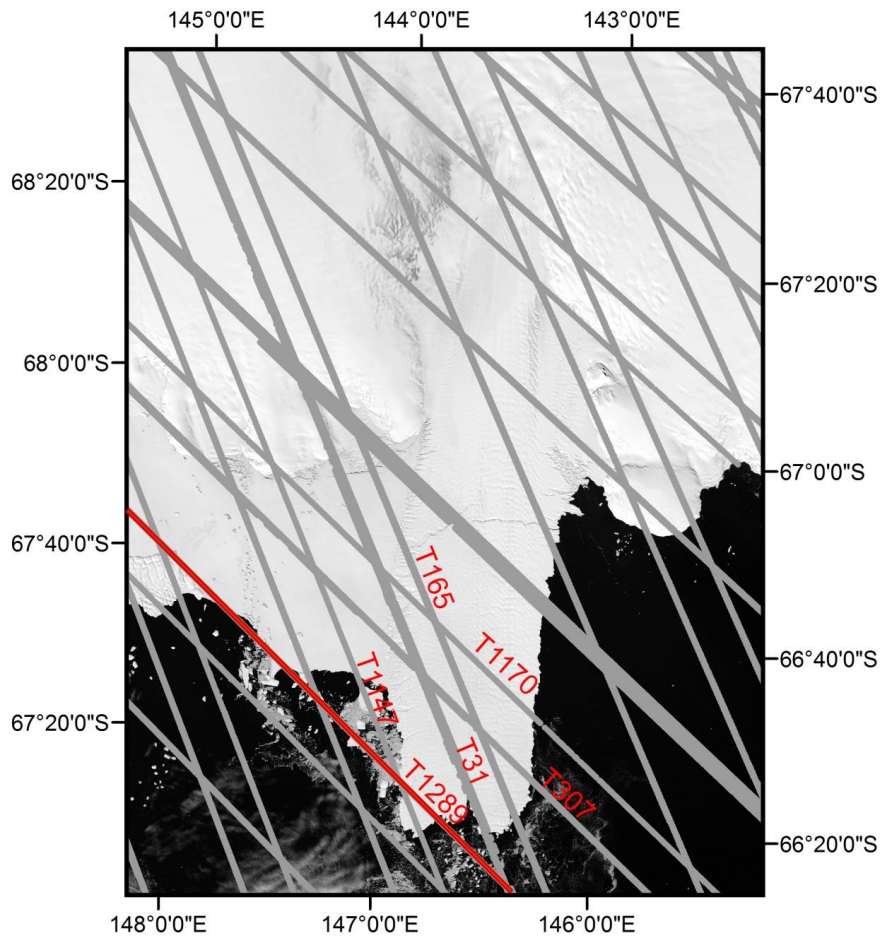
815 |

Figures



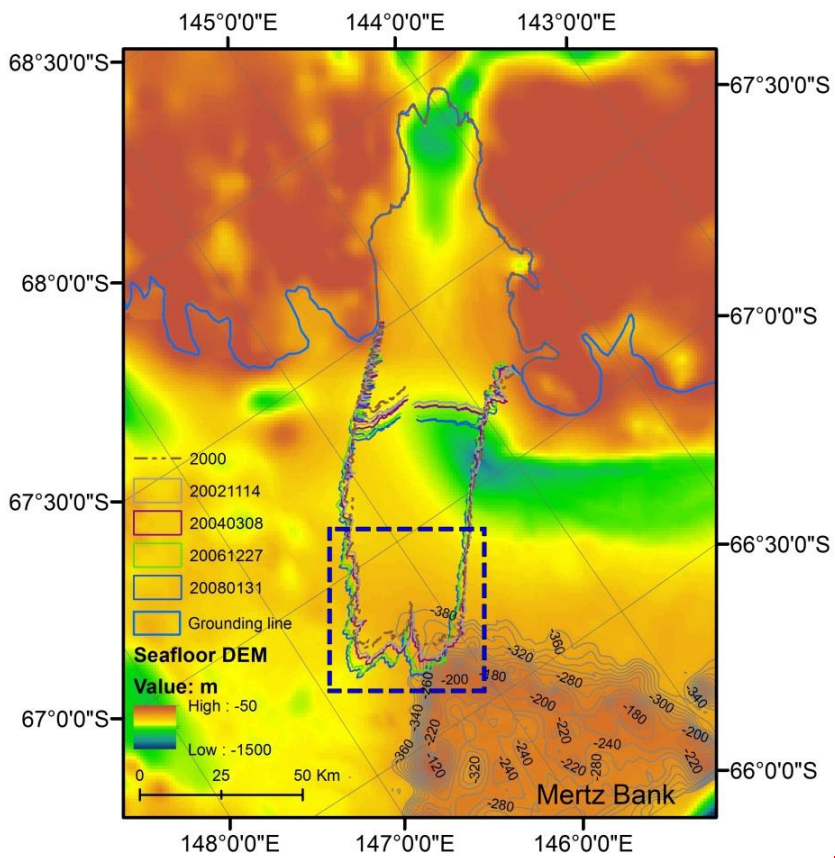
817

818 **Figure 1.** Mertz Ice Tongue (MIT), East Antarctica. Landfast sea ice is attached to the east flank
 819 of the MIT and the Mertz Polynya is to the west. The background image is from band 4 Landsat
 820 7, captured on February 2, 2003. The green square found in the upper left inset indicates the
 821 location of the MIT in East Antarctica. A polar stereographic projection with -71°S as standard
 822 latitude is used.

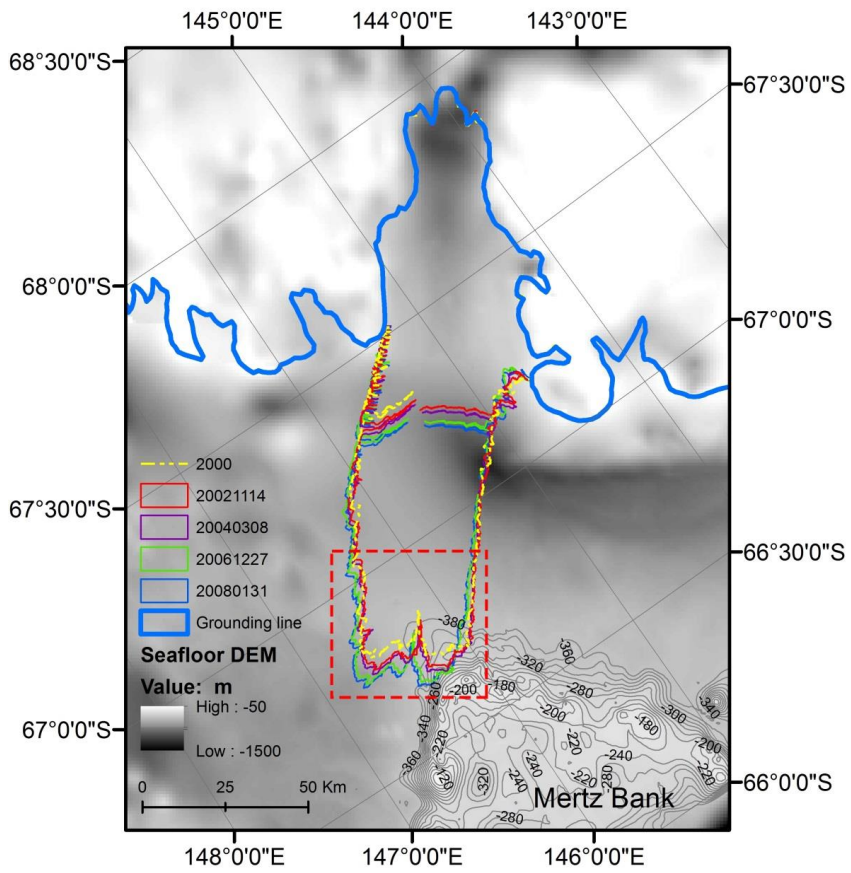


824

825 **Figure 2.** Spatial distribution of ICESat/GLAS data from 2003 to 2009 covering the Mertz
 826 region. Ground tracks of ICESat/GLAS are indicated with gray lines. Track 1289 (T1289) is
 827 highlighted in red as is used in Fig. 4. The background image is from band 4 Landsat 7, captured
 828 on February 2, 2003. A polar stereographic projection with -71 °S as standard latitude is used.



829

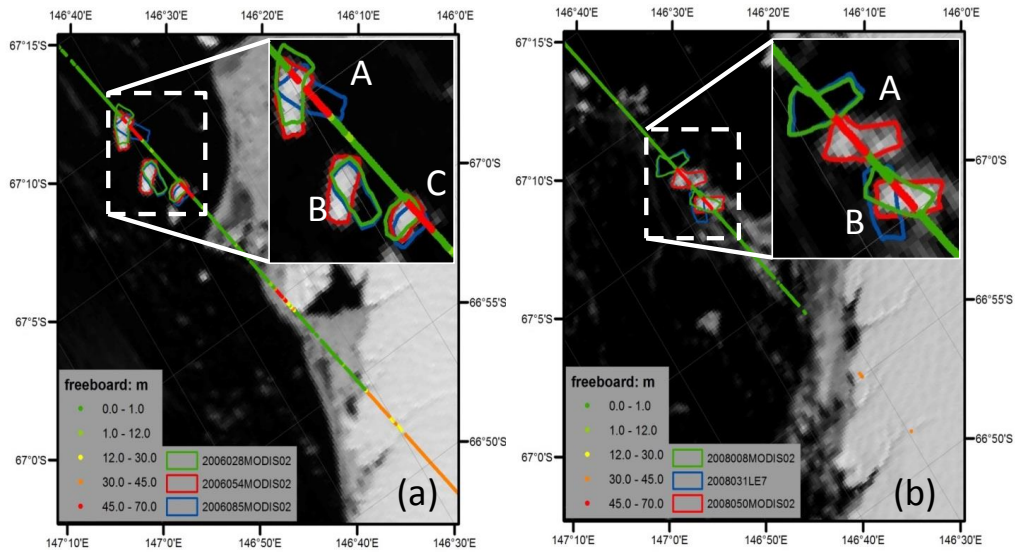


(a)

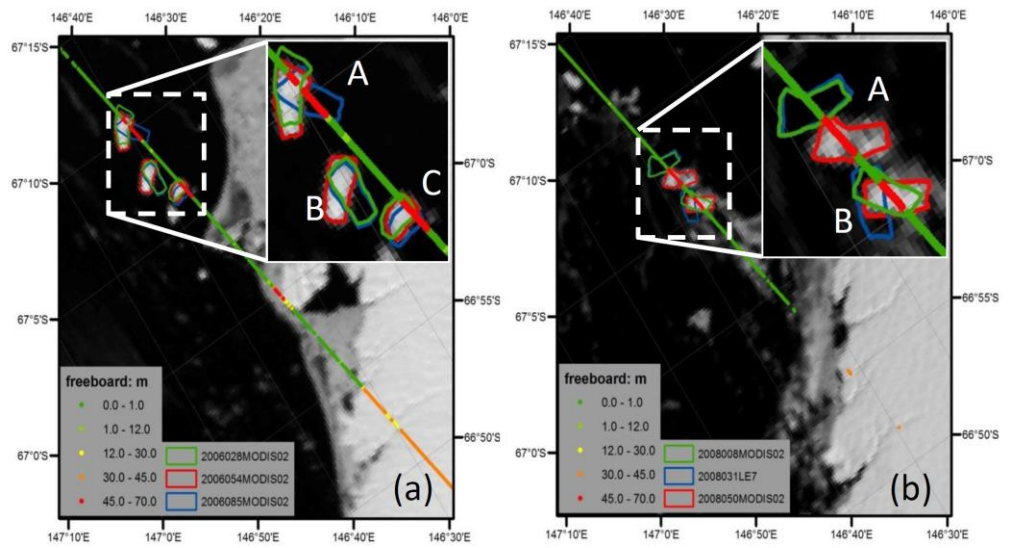
830

831

837 **Figure 3.** (a) Seafloor topography from bathymetry around Mertz region and outlines of the
838 MIT from 2002 to 2008. The outlines of the MIT in different years are marked with different
839 colored polygons. The shallow Mertz Bank is located in the lower right (northeast). The yellow
840 dash-dotted line indicates the shape of the MIT on January 25, 2000, which is used to identify
841 the bathymetry gap under the ice tongue. The ~~dash-dotted blue-red~~ inset box corresponds to
842 location of Figs. 6 and 7. (b) ~~The bathymetry measurement profile can be found from S Fig. 1;~~
843 multi-beam bathymetry dataset coverage over the Mertz region. The embedded figure in the
844 lower left is the zoom in of the red rectangle which shows the positions of iceberg ‘A’ and ‘B’
845 (polygon filled in red) on February 19, 2008 (Fig. 4). (c): single-beam bathymetry dataset
846 coverage over the Mertz region. Blue polylines show the contours around the Mertz Bank and
847 black dots are measurement profiles. (b) and (c) are redrawn from Beaman et al. (2011) because
848 original spatial coverage of the single and multi-beam bathymetry data is not available. However,
849 for being able to use the Figures from Beaman et al. (2011), we geo-registered it and put the
850 contour around Mertz Bank and location of icebergs used in the text over it, from which the
851 density of bathymetry measurement can be clear. From the coastline from Radarsat Antarctic
852 Mapping Project-2000 indicated with the thick gray line in (b) and (c), we can conclude that the
853 geo-registration is successful as it coincides with that from Beaman et al. (2011) well in most
854 parts. This Figure is under a projection of polar stereographic projection with -71 °S as standard
855 latitude.



856



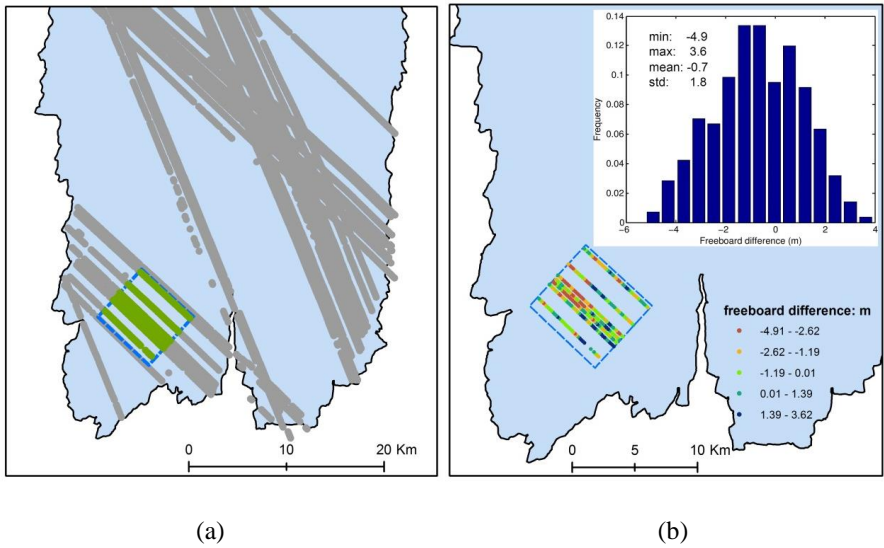
857

858 **Figure 4.** Freeboard extracted from Track 1289, ICESat/GLAS, the location of which can be
 859 found in Fig. 2 and S-Fig. 43(b). (a) and (b) show the freeboard extracted from ICESat/GLAS on
 860 February 23, 2006 (2006054) and February 18, 2008 (2008049) respectively. In each image,

861 positions of three icebergs (with name labeled as 'A', 'B' and 'C') closest to ICESat/GLAS
862 observation time are plotted with green, red and blue polygons respectively. The dates are
863 indicated with seven numbers (yyyddd) in legend. 'yyyddd' stands for day 'ddd' in year
864 | 'yyyy'. 'MODIS02' and 'LE7' ~~indiate~~indicate that ~~the~~ image used to ~~extract~~extract iceberg
865 outline is from MODIS and Landsat 7 ETM+, respectively.

866

867

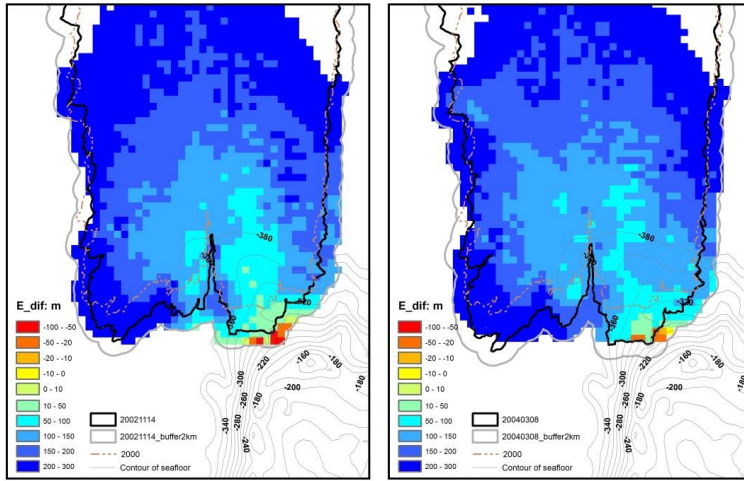


870 **Figure 5.** Evaluation of kriging interpolation method over the MIT using freeboard data derived
871 from ICESat/GLAS. (a) shows profile locations of freeboard derived from ICESat/GLAS after
872 relocation over the MIT. Gray dots indicate ICESat/GLAS used for interpolation using kriging
873 method. The blue dashed square indicates the region used to investigate interpolation accuracy of
874 kriging method, about 7 km \times 7 km. Inside of the square, freeboard data marked with green dots
875 are used to check the accuracy of freeboard interpolated with kriging. (b) is the freeboard
876 comparison result derived by subtracting krigged freeboard from freeboard derived from
877 ICESat/GLAS. The spatial distribution and the histogram of freeboard difference are shown in
878 the lower left and upper right respectively. The black polygon filled with light blue shows the
879 boundary of MIT on November 14, 2002.

880

881

882

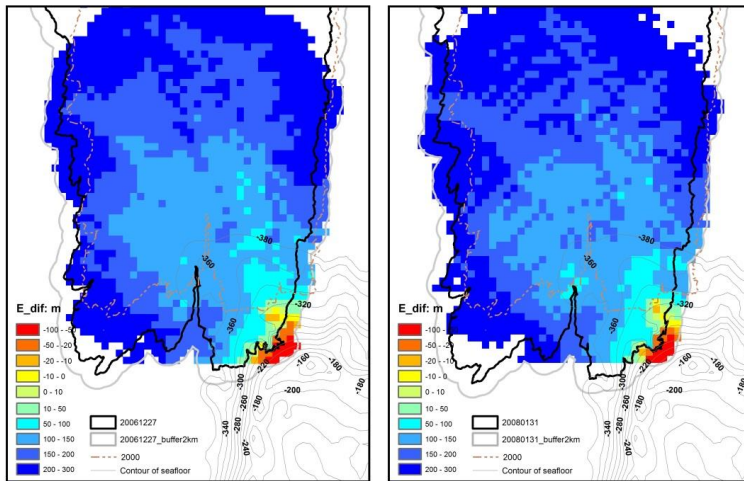


883

884

(a)

(b)



885

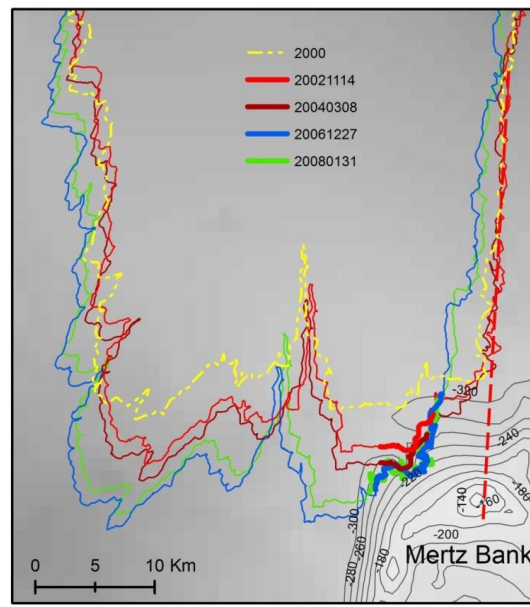
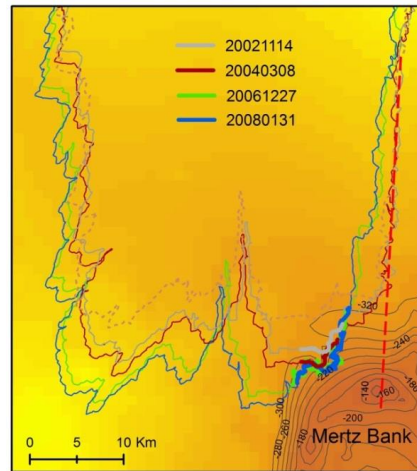
886

(c)

(d)

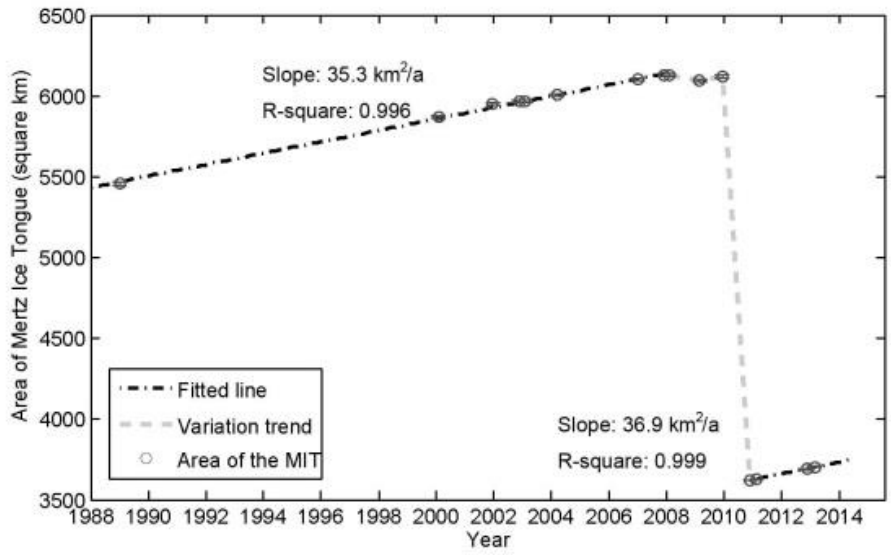
887 **Figure 6.** Elevation difference of Mertz ice bottom and seafloor topography. (a), (b), (c) and (d)
888 correspond to elevation difference assuming hydrostatic equilibrium under the minimum sea
889 surface height -3.35 m on November 14, 2002 , March 8, 2004, December 27, 2006, and January

890 31, 2008, respectively. The contours in the lower right indicate seafloor topography (unit: m) of
891 the Mertz Bank with an interval of 20 m. The solid black line indicates the boundary of the MIT
892 and the thick gray line outlines a buffer region of the boundary with 2 km as buffer radius. The
893 dash-dotted line indicates the shape of the MIT on January 25, 2000, which is used to identify
894 the bathymetry gap under the ice tongue. In the legend, negative values mean that ice bottom is
895 lower than the seafloor, which of course is impossible. Therefore, the initial assumption of a
896 floating ice tongue was incorrect in those locations (yellow to red colors), and the ice was
897 grounded. Regions with more negative values indicate more heavily grounding inside of the MIT
898 or more heavily grounding potential in the buffer region.



902 **Figure 7.** Digital Elevation Map (DEM) of seafloor around Mertz and grounding section of the
903 boundaries extracted from 2002 to 2008. The grounding sections of the MIT boundary in 2002,

904 | 2004, 2006 and 2008 is marked with thick ~~gray~~red, purple, green and blue polylines respectively
905 | and MIT boundaries are indicated with polygons with the same legend as Fig. 3a. Additionally,
906 | MIT boundary in 2000 indicated with dash-dotted yellow polygon is used to show the different
907 | quality of seafloor DEM. Inside of this polygon no bathymetry data was collected or used. The
908 | dashed red line indicates the ‘extension line’ of the west flank of MIT on November 14, 2002,
909 | passing the shallowest region of the Mertz Bank (about -140 m).

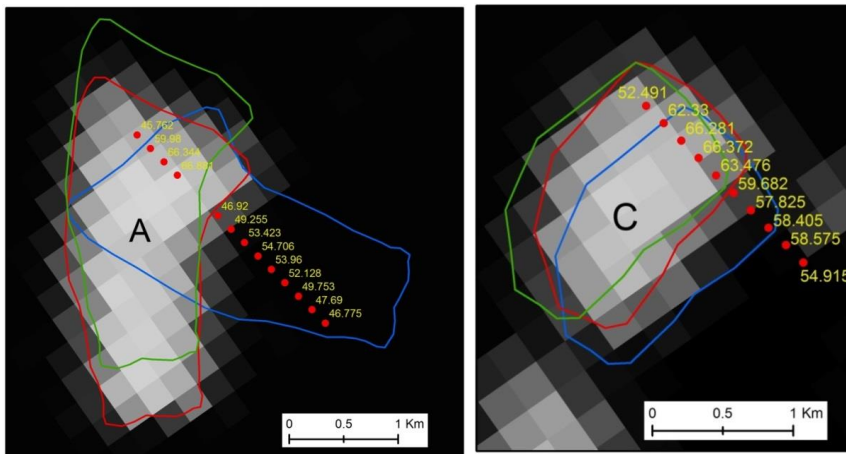


910

911 **Figure 8.** Time series of area change of the MIT. The area covers the entire ice tongue, to the
 912 | grounding line as indicated with thick blue line in Fig. 3a. The area is extracted from Landsat
 913 | images from 1988 to 2013.

914

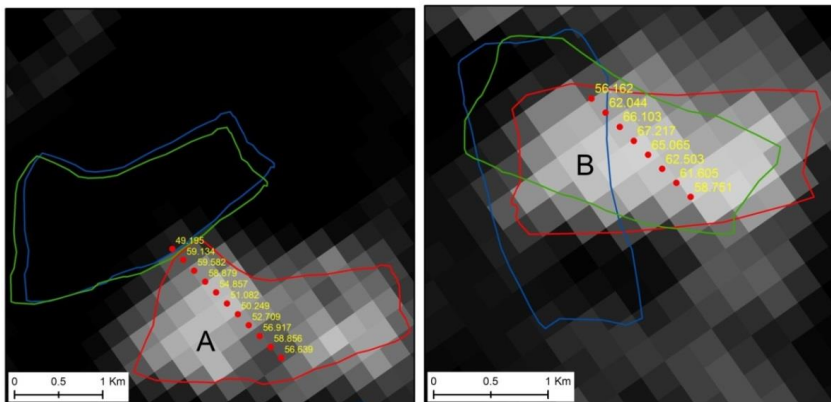
915



916

917

(a) ————— (b)



918

919

(c) ————— (d)

920 **Figure 9.** Freeboard extraction results from ICESat/GLAS for icebergs ‘A’, ‘B’ and ‘C’ in 2006
921 and 2008 respectively. (a) and (b) correspond to freeboard measurements from ‘A’ and ‘C’
922 respectively on February 23, 2006 (2006054), with background image from MODIS captured on
923 2006054. (c) and (d) correspond to freeboard measurements from ‘A’ and ‘B’ respectively on
924 February 18, 2008 (2008049), with background image from MODIS captured on 2008050. The

925 | ~~location of each iceberg in different observation time is indicated with different colored polygons,~~
926 | ~~the legend of which is the same as what is used in Fig. 4. Inside of each sub figure, different~~
927 | ~~icebergs are marked with capital characters 'A', 'B' and 'C' respectively and iceberg freeboard~~
928 | ~~results in unit of meter are marked in yellow.~~

929

930

Tables

931 **Table 1.** Statistics of the ~~three~~ icebergs used to inverse FAC with least-square method and
 932 validation of grounding iceberg detection using this FAC. Icebergs ‘A’, ‘B’ and ‘C’ are the same
 933 as what are used in Fig. 4 and S-Fig 19. Measurements from icebergs ‘A’ and ‘C’ in February
 934 2006 are used to derive FAC with least-squares method. Icebergs ‘A’ and ‘B’ in 2008 are used
 935 for validation.

Icebergs	date	Latitude (°)	Longitude (°)	Freeboard (m)	Seafloor (m)	Sea	ϵ (m)	E_{diff} (m)
						levelSea surface height (m)		
A	Feb 23, 2006	-67.1737	146.6595	66.88	-528.48	-1.92	0.89	
		-67.1752	146.6604	66.34	-527.01	-1.92	1.30	
C	Feb 23, 2006	-67.1085	146.6247	66.37	-505.84	-1.92	-	1.25
		-67.1100	146.6255	66.28	-507.08	-1.92	-	1.01
A	Feb 18, 2008	-67.1194	146.6303	58.88	-522.52	-2.08		69.14
		-67.1209	146.6311	59.58	-524.16	-2.08		64.88
B	Feb 18, 2008	-67.0906	146.6151	67.22	-500.92	-2.08		-
		-67.0921	146.6159	66.10	-500.47	-2.08		22.45
								-
								13.55

936

937 **Table 2.** Statistics of grounding grids inside or grounding potentials outside of the Mertz Ice
 938 Tongue (MIT) (‘I’: inside of thick black line, Fig. 6; Number in brackets indicates how many
 939 grids are located inside of the 2000 Mertz boundary; ‘O’: between the black and gray lines, Fig.
 940 6) on November 14, 2002, March 8, 2004, December 27, 2006 and January 31, 2008 respectively.
 941 Each grid covers an area of 1 km². The Mean, Minimum and Standard deviation is calculated
 942 without considering those fallen inside of the 2000 Mertz boundary, but only those having
 943 elevation difference less than 46 m and out of 2000 Mertz boundary.

944

Elevation difference (subtracting seafloor from ice bottom)	2002-11-14		2004-03-08		2006-12-27		2008-01-31	
	I	O	I	O	I	O	I	O
23-46 (m)	9(3)	10(0)	6(0)	3(0)	10(1)	1(0)	10(3)	5(0)
0-23 (m)	2(0)	6(0)	1(0)	1(0)	9(0)	2(0)	4(0)	2(0)
<0 (m)	0(0)	8(0)	2(0)	5(0)	7(0)	21(0)	6(0)	18(0)
Mean (m)	28.8	9.8	15.8	-1.1	10.9	-41.9	12.3	-31.0
Minimum (m)	11.9	-81.5	-46.0	-44.5	-52.3	-102.8	-34.8	-103.0
Standard deviation (m)	9.2	36.8	29.6	31.4	24.7	37.6	27.3	38.0
Number of grids	8	24	9	9	25	24	17	25

945

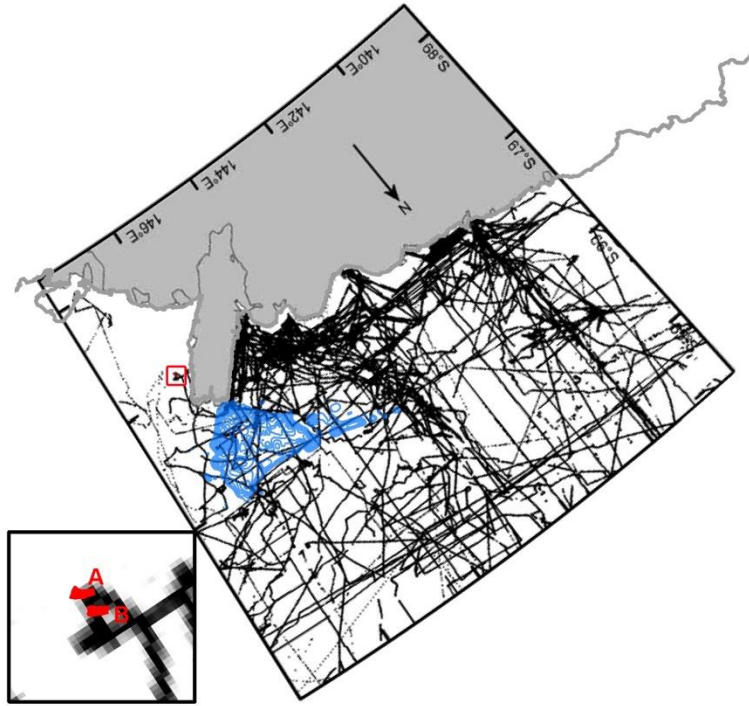
946 **Table 3.** Statistics of grounding outlines of the MIT as shown with thick polylines in Fig. 7 on
 947 November 14, 2002, March 8, 2004, December 27, 2006 and January 31, 2008 respectively

	2002-11-14	2004-03-08	2006-12-27	2008-01-31
Start location (°)	146.124 °E, 66.696 °S	146.155 °E, 66.681 °S	146.093 °E, 66.700 °S	146.088 °E, 66.699 °S
End location (°)	146.240 °E, 66.693 °S	146.256 °E, 66.683 °S	146.304 °E, 66.669 °S	146.292 °E, 66.668 °S
Perimeter (km)	7.0	6.4	24.7	20.9

948

1

Supplementary Figures



2

3

(a)



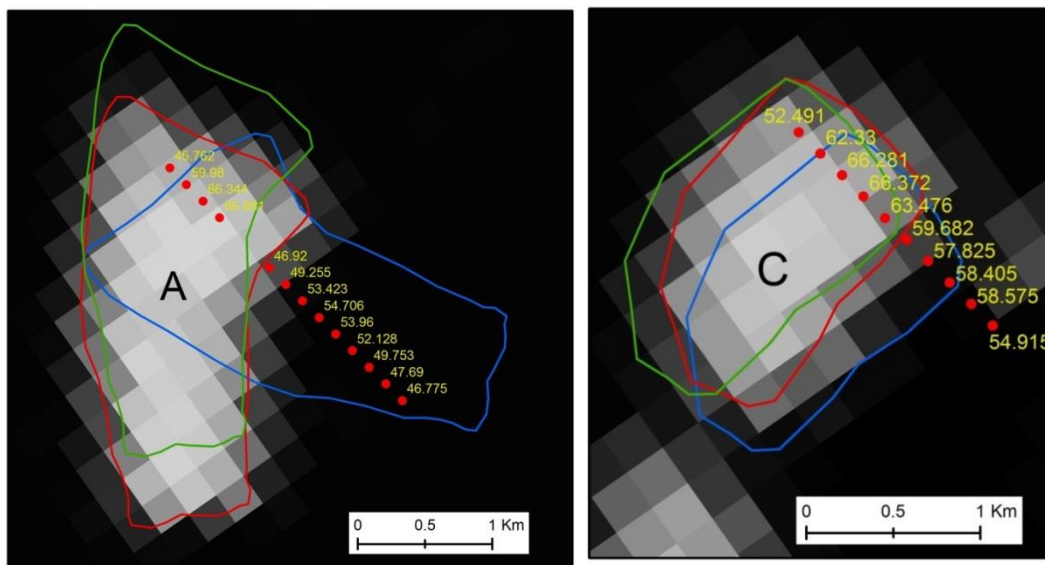
4

5

(b)

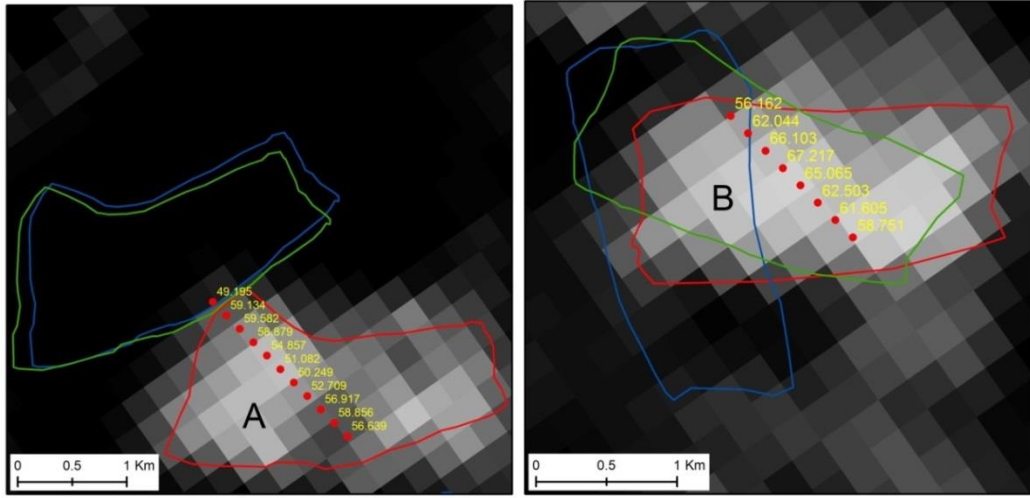
6 ~~S-Figure 1. Bathymetric measurement profiles covering the Mertz region. (a): multi-beam~~
7 ~~bathymetry dataset coverage over the Mertz region. The embedded figure in the lower left is the~~
8 ~~zoom in of the red rectangle which shows the positions of iceberg 'A' and 'B' (polygon filled in~~
9 ~~red) on February 19, 2008 (Fig. 4). (b): single-beam bathymetry dataset coverage over the Mertz~~
10 ~~region. Blue polylines show the contours around the Mertz Bank and black dots are measurement~~
11 ~~profiles. The Figure is redrawn from Beaman et al. (2011) because original spatial coverage of~~
12 ~~the single and multi-beam bathymetry data is not available. However, for being able to use the~~
13 ~~Figures from Beaman et al. (2011), we geo-registered it and put the contour around Mertz Bank~~
14 ~~and location of icebergs used in the text over it, from which the density of bathymetry~~
15 ~~measurement can be clear. From the coastline from Radarsat Antarctic Mapping Project 2000~~
16 ~~indicated with the thick gray line, we can conclude that the geo-registration is successful as it~~
17 ~~coincides with that from Beaman et al. (2011) well in most parts. The Figure is under a~~
18 ~~projection of polar stereographic projection with 71°S as standard latitude.~~

19



21

(a) (b)



22

(c) (d)

23

24

25

26

27

28

29

30

31

32

33

S-Figure 1. Freeboard extraction results from ICESat/GLAS for icebergs ‘A’, ‘B’ and ‘C’ in 2006 and 2008 respectively. (a) and (b) correspond to freeboard measurements from ‘A’ and ‘C’ respectively on February 23, 2006 (2006054), with background image from MODIS captured on 2006054. (c) and (d) correspond to freeboard measurements from ‘A’ and ‘B’ respectively on February 18, 2008 (2008049), with background image from MODIS captured on 2008050. The location of each iceberg in different observation time is indicated with different colored polygons, the legend of which is the same as what is used in Fig. 4. Inside of each sub-figure, different icebergs are marked with capital characters ‘A’, ‘B’ and ‘C’ respectively and iceberg freeboard results in unit of meter are marked in yellow.